REFERENCE COPY

[redacted]

UNCLASSIFIED

NATIONAL AERONAUTICS AND SPACE ADMINISTRATION

Space Programs Summary No. 37-39, Volume II

for the period March 1, 1966 to April 30, 1966

The Planetary–Interplanetary Program

(Title Unclassified)

482

JET PROPULSION LABORATORY
LIBRARY

JUL 8 1966

Copy No._____

CALIFORNIA INSTITUTE OF TECHNOLOGY

JET PROPULSION LABORATORY
CALIFORNIA INSTITUTE OF TECHNOLOGY
PASADENA, CALIFORNIA

May 31, 1966

Classification Changed to UNCLASSIFIED
Authority JPL-Letter to NASA-Langley on Nov. 4, 1970, signed by W.E. Hanson
Date Jan. 4, 1971 By Q. Carstairs

LAB-C01310

[redacted]
GROUP 4 ... declassified after 12 ...

UNCLASSIFIED

149154

UNCLASSIFIED

Preface

The *Space Programs Summary* is a six-volume, bimonthly publication that documents the current project activities and supporting research and advanced development efforts conducted or managed by JPL for the NASA space exploration programs. The titles of all volumes of the *Space Programs Summary* are:

Vol. I. The Lunar Program (Confidential)

Vol. II. The Planetary–Interplanetary Program (Confidential)

Vol. III. The Deep Space Network (Unclassified)

Vol. IV. Supporting Research and Advanced Development (Unclassified)

Vol. V. Supporting Research and Advanced Development (Confidential)

Vol. VI. Space Exploration Programs and Space Sciences (Unclassified)

The *Space Programs Summary,* Vol. VI consists of an unclassified digest of appropriate material from Vols. I, II, and III; an original presentation of technical supporting activities, including engineering development of environmental-test facilities, and quality assurance and reliability; and a reprint of the space science instrumentation studies of Vols. I and II.

W. H. Pickering, *Director*
Jet Propulsion Laboratory

Space Programs Summary No. 37-39, Volume II

Copyright © 1966, Jet Propulsion Laboratory, California Institute of Technology

Prepared under Contract No. NAS 7-100, National Aeronautics & Space Administration

This document contains information affecting the national defense of the United States, within the meaning of the Espionage Laws, Title 18, U.S.C., Sections 793 and 794, the transmission or revelation of which in any manner to an unauthorized person is prohibited by law.

UNCLASSIFIED

UNCLASSIFIED

Contents

I. *Mariner* 1967 Project 1
A. Introduction 1
B. Engineering Mechanics 3
C. Guidance and Control 6
Reference 10

II. *Mariner* Mars 1969 Project 11
A. Introduction 11
B. Systems 11
C. Guidance and Control 12

III. *Voyager* Project 14
A. Introduction 14
B. Project Engineering 15
C. Engineering Mechanics 19
D. Guidance and Control 20
E. Telecommunications 21
References 34

IV. Future Projects 35

UNCLASSIFIED

UNCLASSIFIED

I. *Mariner* 1967 Project

A. Introduction

The *Mariner* 1967 Project continues and extends the work of the previous *Mariner* Projects. Two elements of the Project are concerned with the *Mariner IV* spacecraft now in space, while a third is concerned with the Venus flyby mission in 1967.

1. Mariner *Mars 1964 Project*

Residual activity of the *Mariner* Mars 1964 Project consists primarily of continuing analysis of tracking data, publication of results by the principal investigators, and preparation of final reports. However, periodic detection, recording, and commanding activities involving the *Mariner IV* spacecraft have been assigned to the Deep Space Network (DSN). Using elements of the experimental facilities at Goldstone Station and advanced R&D techniques, attempts will be made to communicate with the spacecraft. Results are published in *SPS*, Vol. III.

2. Mariner IV *Project*

In the second half of 1967, *Mariner IV* will again be within the normal communication range of the DSN stations. At that time an attempt will be made to obtain additional telemetry data from *Mariner IV*. The *Mariner IV* Project comprises the preparation, support, and actual reacquisition of the spacecraft.

The objectives, authorized in December 1965 simultaneously with those for the Venus flight, have been established as follows:

> *The primary objective of the Mariner IV Project is to obtain scientific information on the interplanetary environment in a region of space further from the Sun than the orbit of Earth during a period of increasing solar activity in 1967, using the Mariner IV spacecraft still operating in orbit around the Sun.*
>
> *The secondary objectives are to obtain additional engineering knowledge about the consequences of extended exposure of spacecraft equipment in the interplanetary space environment and to acquire experience in the operation of a planetary spacecraft after a prolonged lifetime in deep space.*

Flight operations on this project (providing a functioning spacecraft allows this to occur) will overlap the *Mariner* Venus 67 Project flight activities.

UNCLASSIFIED

UNCLASSIFIED

3. Mariner *Venus 67 Project*

The major task of the *Mariner* 1967 Project is the Venus flyby mission, named the *Mariner* Venus 67 Project. The following mission objectives have been established:

> *The primary objective of the Mariner Venus 67 Project is to conduct a flyby mission to Venus in 1967 in order to obtain scientific information which will complement and extend the results obtained by Mariner II relevant to determining the origin and nature of Venus and its environment.*
>
> *Secondary objectives are to acquire engineering experience in converting and operating a spacecraft designed for flight to Mars into one flown to Venus, and to obtain information on the interplanetary environment during a period of increasing solar activity.*

With the authorizing of this project late in December of 1965, and the launch opportunity occurring in June 1967, the period available to the *Mariner* Venus 67 Project for planning, design, test, and other flight preparation is 18 mo. Because of this minimum length of time, application, to the fullest extent possible, must be made of techniques developed from the experience of prior missions, and existing hardware must be utilized.

The single flight spacecraft, designated M67-2, is currently being prepared by converting the spare spacecraft (MC-4) that was built for the *Mariner* Mars 1964 Project.[1]

[1]Portions of the proof-test model (PTM) spacecraft and spares from the MM64 Project are also being prepared as a flight-support spacecraft (M67-1); there will be no PTM as such. The flight-support spacecraft will serve the double function of pseudo-PTM and backup spacecraft for qualifying spare subsystems.

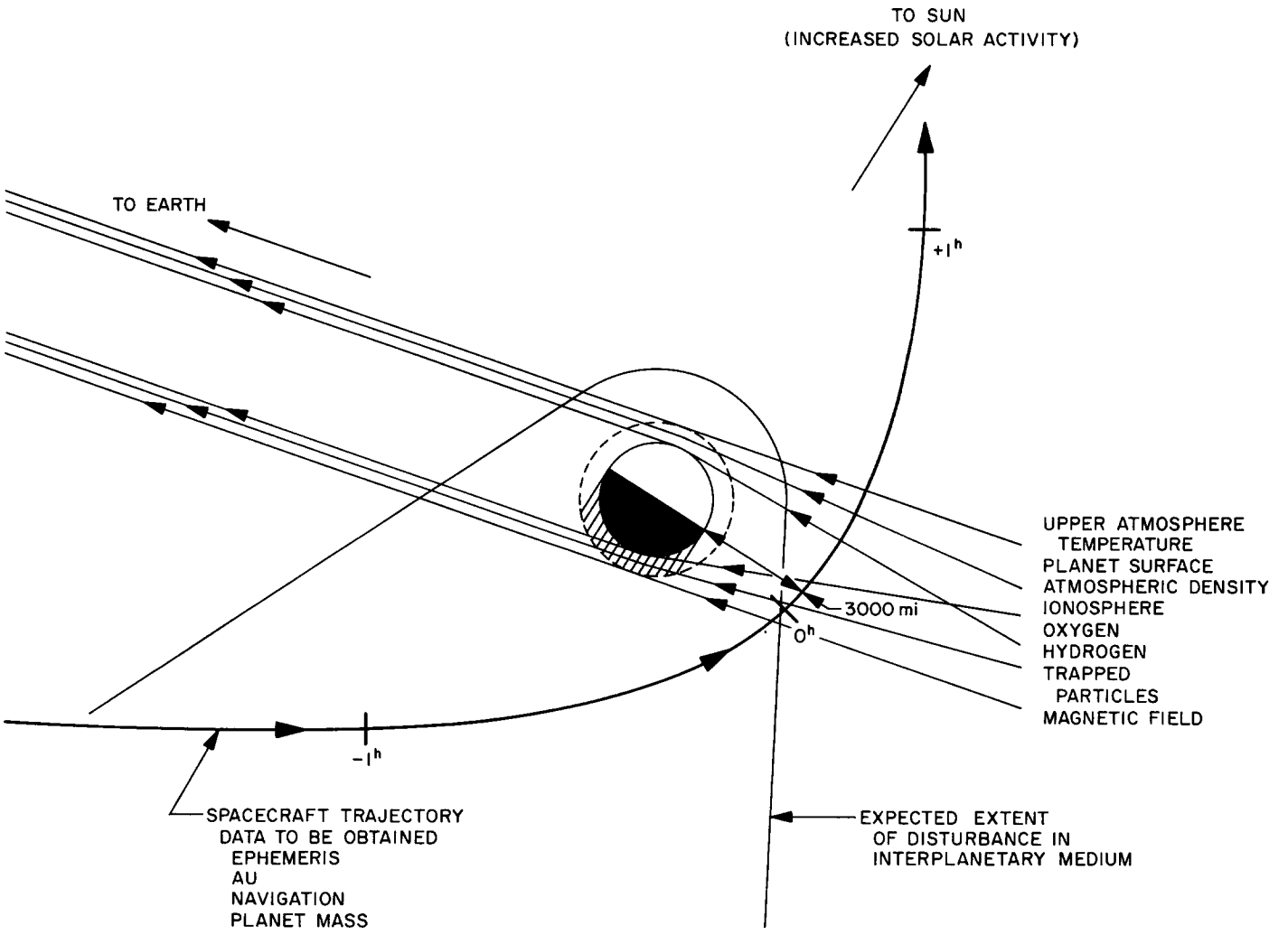

Fig. 1. *Mariner* Venus 67 encounter science

UNCLASSIFIED

UNCLASSIFIED

An *Atlas-Agena D* launch vehicle will inject the spacecraft into a 120-day transit trajectory. The launch readiness date has been set at June 10, 1967, with a 14-day launch period starting June 12. Ranging provisions have been authorized for this mission which will offer the possibility of considerably enhancing the celestial mechanics experiment. At encounter, an unusually sharp perturbation will occur. Fig. 1 depicts this perturbation and also lists the scientific data to be obtained on this mission.

Seven scientific experiments have been approved for the *Mariner* Venus 67 mission:

Experiment	*Principal investigator*
S-Band radio occultation	Arvydas J. Kliore, Jet Propulsion Laboratory
Ultraviolet photometer	Charles A. Barth, University of Colorado
Dual-frequency radio propagation	Von R. Eshleman, Stanford University
Helium magnetometer	Edward J. Smith, Jet Propulsion Laboratory
Solar plasma	Herbert S. Bridge, Massachusetts Institute of Technology
Trapped radiation	James A. Van Allen, State University of Iowa
Celestial mechanics	John D. Anderson, Jet Propulsion Laboratory

The first experiment requires the use of only the RF transmission subsystem on the spacecraft, and the last one utilizes only the tracking doppler data derived from the RF carrier. Of the remaining five experiments, four are to be accomplished with the existing instrumentation, with only minor modifications. Only the dual-frequency radio propagation experiment of Stanford requires the incorporation of a new scientific instrument into the payload.

Other changes to the basic spacecraft design are necessitated by the fact that the spacecraft will travel toward, rather than away from, the Sun and also because conversions must be made to accommodate revised encounter sequencing and science payload. In particular, modifications are needed in the following areas:

(1) Scientific data automation system

(2) Antenna pattern and orientation

(3) Thermal control

(4) Solar panel configuration

(5) Planetary sensors

In this reporting period all major posts were filled, and staffing assignments were made. The preliminary design of the spacecraft was completed, but many details of engineering and mechanization remain to be resolved. The integration of *Mariner IV* and *Mariner* Venus 67 flight operations is being studied. As protection against a disaster on the launch pad, both Launch Complexes 12 and 13 at Cape Kennedy will be prepared.

B. Engineering Mechanics

1. Introduction

The preliminary design of the *Mariner* Venus 67 spacecraft (M67-2) has been completed. Detailed design definition is continuing in the structures, mechanical devices, electronic packaging, cabling, and temperature-control areas. Electronic part requirements from the electronic subsystems are being defined, and part procurement and screening activities are proceeding. A single screening contract for the bulk of the parts procured has been issued.

The solar panel structure and boost damper design is completed. The basic design, fabrication, and temperature control techniques are similar to those of *Mariner C*. A dynamic test of the design approach, using *Mariner C* solar panels and prototype dampers, verified that the design approach is sound.

2. Electronic Parts Acquisition

When the decision was made in December 1965 to plan a *Mariner* spacecraft for a flight to Venus in 1967, there was insufficient lead-time to buy Hi-Rel or preferred parts. The solution chosen was to buy components which had exhibited reliable characteristics in the past and to test these parts mechanically and electrically to screen out the inferior ones.

UNCLASSIFIED

UNCLASSIFIED

This decision called for a large-scale parts screening program. Experience pointed out two problems associated with screening: (1) maintaining close technical liaison over the screening agencies, and (2) monitoring and controlling screening status and scheduling. A single vendor was chosen to screen capacitors, diodes, resistors, and transistors; another vendor was selected to screen the small quantity of transformers. JPL parts quality assurance (PQA) is screening special part types: fuses, cells, relays, and small quantities of all the above-mentioned part types.

The theory behind contracting a single major screening vendor has proven sound in that it has been possible to control the contract with a minimal number of JPL personnel. This is in striking contrast to the *Mariner IV* effort where 14 screening agencies were involved, with the attendant demand for considerable JPL monitoring.

3. Solar Panel Design

a. Configuration. The M67-2 solar panel configuration has followed as closely as possible the previous *Mariner C* configuration. The approach has been to minimize the number of changes in interfaces between the panel structure and interacting systems, while still satisfying the area temperature-control, and structural dynamics requirements of the Venus mission.

The solar panel configuration for M67-2 involves four solar panels mounted to the same hinge points as *Mariner C* panels, but attached to each other at the tips during boost, rather than being attached to the antenna support structure as on *Mariner C*. The back beam structure for the panels is the same as *Mariner C*, except for two brackets at the tips and an added set of cross-braces about halfway up the back beams. Retaining the *Mariner C* back beam structure makes possible the utilization of *Mariner C* attitude-control gas systems, solar panel cruise dampers, solar panel actuators, and solar panel open switches with no design modifications. The corrugated substrate design from *Mariner C* is also used on the new panel; however, the corrugation aluminum foil thickness has been raised from 3.5 to 5.0 mils in order to increase structural reliability and reduce the possibility of handling damage. Because the spacecraft will travel toward the Sun, the corrugations are mounted on the side of the spars opposite that of the *Mariner C* panel. This change results in some rerouting of panel power cabling and in moving the diode mounting surface to the side opposite that of *Mariner C*'s panel back beam.

b. Adhesives. All adhesives used in the *Mariner C* panel have been requalified for use at the elevated temperatures encountered by the M67-2 panels. Some of these are permanently degraded in strength after extensive aging at temperatures greater than 300°F; however, high-temperature aging is no problem, since it occurs in the flight sequence after the high stresses of launch.

c. Damping. The primary structural innovation made on the solar panels is the use of tip latching to interconnect them during boost. This scheme clears the center area of the bus structure by removing the need for panel support struts, thus decoupling (to a greater extent) the design of the panels from that of the antenna system.

The panels are interconnected through damped struts which absorb vibrationally induced energy, thereby preventing the buildup of damaging structural resonances. The location of these dampers at the panel tips gives them positive control of more panel resonances than did the *Mariner C* configuration while using smaller, lighter dampers.

d. Deployment. The tip-latched panels are deployed by actuating four pinpullers rather than the eight required on *Mariner C*; however, if any single pinpuller fails to actuate, two panels will remain undeployed rather than one. As in *Mariner C*, all pinpullers must function to release the panels, or the mission will be degraded.

e. Testing. The dynamics of the tip-latched panel configuration have been analyzed and appear to be functional. The analytical techniques and mechanization are new; therefore, a test was run to verify the analysis.

The test hardware consisted of four *Mariner C* panels having dummy cells and modified to include prototype tip latching to verify the suitability of such a latching scheme. The modifications were such that the line of action of the tip spring dampers (Fig. 2) was the same as that for the proposed M67-2 configuration. The four panels were mounted to a slider plate (Fig. 3), and excitation was introduced parallel to two panels and perpendicular to the other two. The attitude-control jets and cabling were not simulated. The configuration was tested at various levels up to the *Mariner C* structure type-approval dynamic test level in the lateral direction. Additional tests were conducted at an angle of 45 deg to the panels, but a defective damper was detected for that portion of the test, which resulted in data of questionable value.

The test results are compared with analytical results in Fig. 4. The analytical model was based on a four-panel

UNCLASSIFIED

UNCLASSIFIED
CONFIDENTIAL

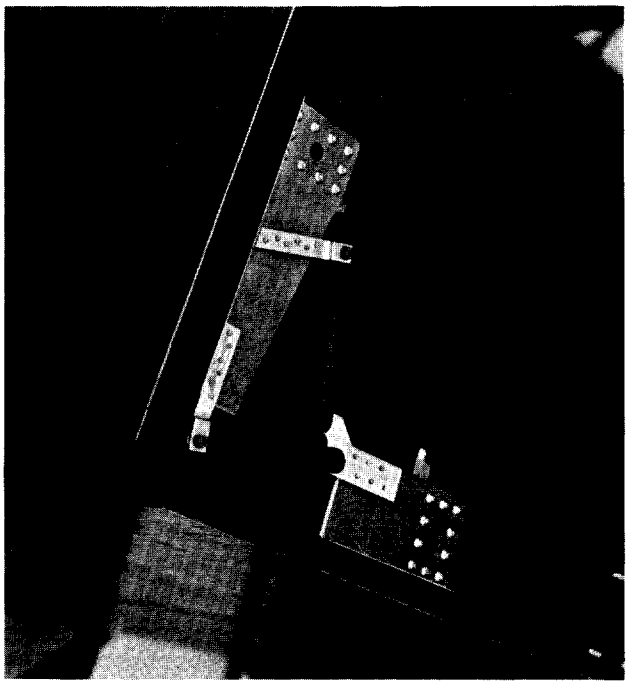

Fig. 2. Prototype boost dampers installed on solar panel

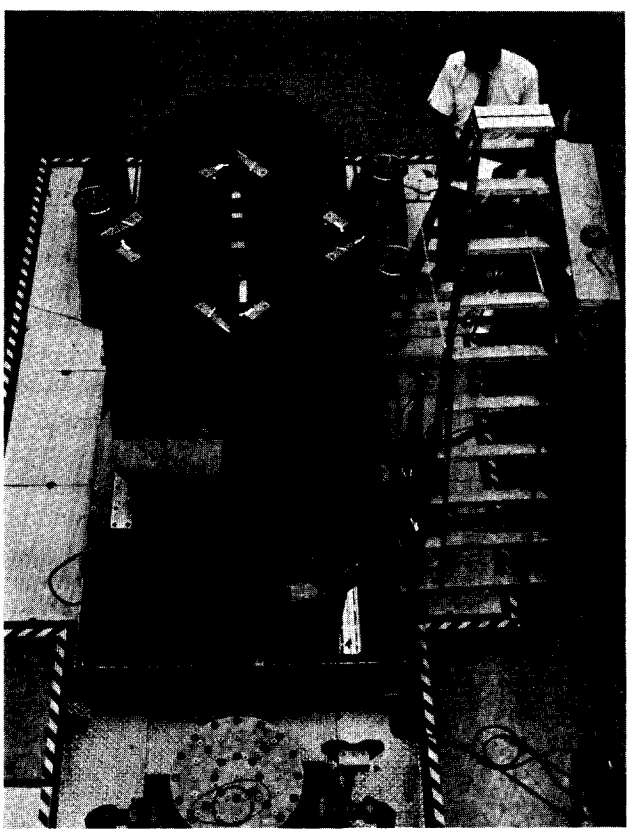

Fig. 3. Solar panel damper vibration test setup

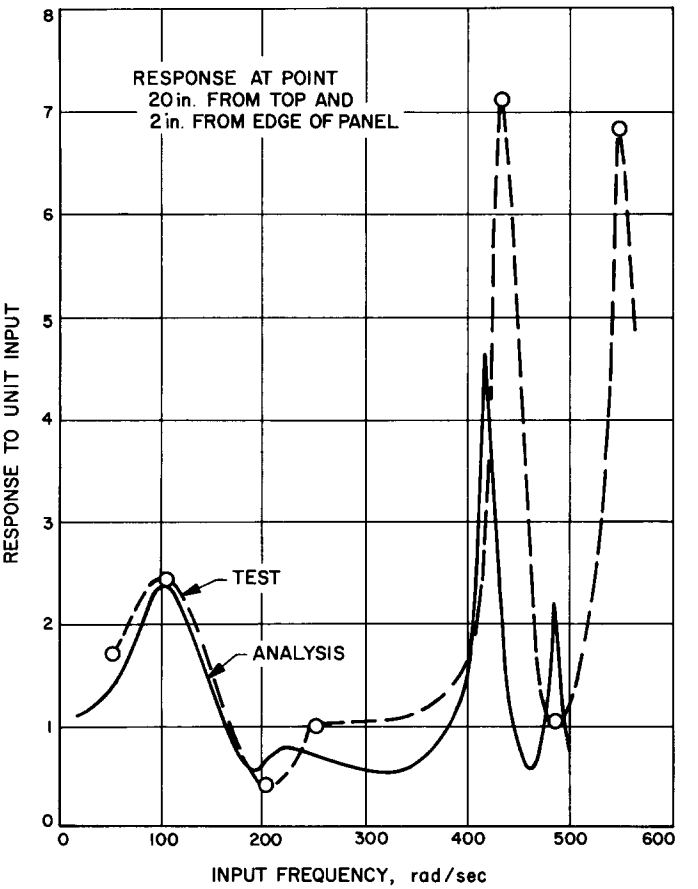

Fig. 4. Response of tip-latched *Mariner C* solar panels to unit acceleration

configuration with in-plane interconnecting spring-damper loads applied at the shear centers of the panels. The test model had these loads applied 2 to 4 in. from the shear center. The analytic model had the panels vertical, whereas the test model had the panels sloping inward approximately 3½ deg. The modal damping of the analytic model was assumed to be 1.0% for all modes, except the in-plane mode. This is approximately the average of that measured in the M67-2 configuration. There has been no modal test performed on the M67-2 configuration, but the in-plane modal damping was measured during a single *Mariner C* panel test, both by log decrement tests and the half-power-point method and the measured value of 0.3% was used in the analysis. The method of analysis is such that good results can be expected only at frequencies below 80 cps. The values plotted as test values in Fig. 4 are the ratio of the output amplitude to input amplitude after both have been processed to retain only their fundamental acceleration content. The comparison between analysis and test is very favorable at low frequencies, as was expected.

CONFIDENTIAL
UNCLASSIFIED

UNCLASSIFIED

Frequency prediction is seen to be quite good at the higher frequencies, but the response prediction is low. This is very sensitive to the structural damping coefficient used in the analysis and can be much improved by a better approximation of panel structural damping which must be obtained by tests.

f. Dielectric. One *Mariner C* polymer which was not acceptable at elevated temperature was the SMP 62/63 dielectric used on the cell mounting surface. High-temperature testing revealed drastic softening of that material, which made it unacceptable as a mechanical barrier for the Venus mission. An alternate material (Epon 956) has been selected which does not soften at high temperature and which can be sprayed onto the panel just as the original dielectric was. As the panel surface is sprayed with Epon 956, a layer of 2-mil glass cloth is laid into the resin, thereby placing a mechanical spacer between the solar cells and the panel surface. The glass cloth also simplifies visual inspection of the dielectric thickness by presenting an unwet appearance when too little resin is used. High-temperature penetration tests indicate that the Epon 956 and fiberglass dielectric is very suitable for the Venus mission, and a weight study indicates virtually no weight penalty over the *Mariner C* panel design.

g. Temperature Control. The M67-1 solar panel temperature control scheme is essentially unchanged from that of the *Mariner C* panel; every effort is being made to keep the panel as cool as possible. The back of the panel is painted black to maximize its heat radiation to a hemisphere of space; while the front, being covered with dark cells, radiates a nearly equal amount of heat to the opposite hemisphere.

Unlike the *Mariner C* panel surface, the new panel's surface is held well away from the spacecraft itself. This minimizes the panel's absorption of spacecraft thermal radiation and reduces the tip-to-base temperature gradient of the panel's celled area.

The temperature-control scheme outlined above is complicated only by the requirement that a series of power dissipation diodes be mounted to the spar in such a way that they can dissipate excess power when the panel is very cold and the cells, therefore, very efficient. The heat-dissipation requirements for the diodes on the Venus mission are less severe than the requirements for *Mariner C* and the heat-dissipation ability of the M67-2 solar panel spar has been improved by bonding, rather than spot-welding, the doublers at the diode mounting holes.

C. Guidance and Control

1. Celestial Sensors

a. Introduction. There are five basic celestial sensors to be used on the *Mariner* Venus 67 mission: (1) Sun sensors, (2) Canopus sensor, (3) Earth sensor, (4) terminator sensor, and (5) planet sensor. The planet sensor is a new device, and the remaining ones are modifications of those of the *Mariner C*.

b. Sun sensors. The Sun sensors to be used on *Mariner* Venus will be identical to *Mariner C* sensors, except for a change in excitation voltage to allow for operation at the high illumination levels near Venus.

c. Canopus sensor. The *Mariner* Venus 67 Canopus sensor is a "minimum changes" modification of the *Mariner C* Canopus sensor (Ref. 1). The major change involves reducing the straylight sensitivity by redesigning the optics and shade. Straylight from Venus in 1967 may be as much as sixty times more intense and at a much less favorable angle than the light from Mars in 1964. The widely publicized dust-particle-induced losses of star acquisition will be eliminated by modifying the sensor acquisition gate. Minor modifications to the cone-angle program, the error-signal phasing, and the mounting surface are required to satisfy the mission and configuration constraints.

The straylight problem. The extent of the straylight problem can only be discussed in very preliminary terms, since much of the geometric and illumination analysis is still incomplete. For preliminary purposes, 4,500 ft-c is being used as a design criterion. This is the illumination from a 120-deg angular-diameter disk, whose brightness equals the average brightness of Venus at full phase. This disk is located 30 deg off the optical axis of the Canopus sensor. The actual illumination level from Venus depends on the exact Sun-Venus-Canopus-spacecraft geometry. The worst-case geometry is of primary importance, since the sensor must be designed to operate in this situation. We are currently analyzing this problem and this information will be available for flight-acceptance testing. Aiming points for the Venus mission cause the Canopus-probe-Venus limb angle to be as low as 36 deg. Since the *Mariner C* Canopus sensor would be inoperable for illumination levels on the order of 10 to 30 ft-c at 36 deg from the optical axis, a factor of 150 to 450 improvement is required in the straylight shade.

This order of improvement is readily achieved with a two-staged shade. A two-staged shade has been designed which will give two-stage protection outside a cone which

UNCLASSIFIED

UNCLASSIFIED

is $\pm 41 \times \pm 22$ deg, centered on a 90-deg cone angle and a 0-deg clock angle. Calculations indicate that this shade should easily protect against the lit limb of Venus outside of this constraint. This shade, shown in Fig. 5, extends 4.5 in. in front of the *Mariner C* Canopus sensor and requires a new refracting optical system with a 0.5-in. aperture, and the relocation of the Sun shutter and Sun detector. A prototype is being fabricated from the layout, and the shade will be evaluated while manufacturing drawings and procurement of flight shades is accomplished.

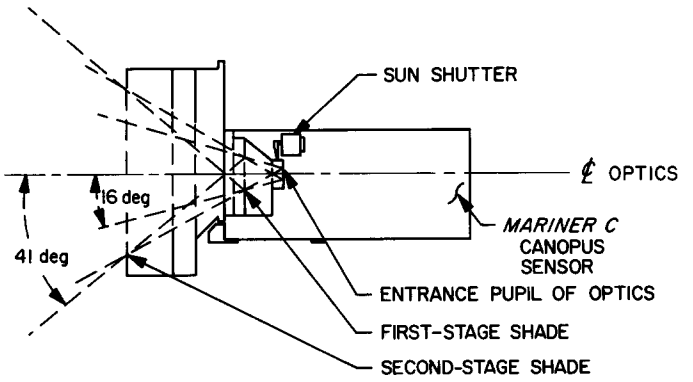

Fig. 5. Preliminary configuration second-stage Canopus sensor shade

The establishment of a facility to test the sensor's response to straylight is complicated by the background sensitivity of the *Mariner C* Canopus sensor. In order to successfully test the sensor, the ambient background light must be less than 1.45×10^{-4} ft-lamberts. For the required illumination, the background brightness of pure dust-free air at STP is 3.85×10^{-3} ft-lamberts. An environment of pure helium would be theoretically capable of reducing the molecular scattering by a factor of 69.5; however, the sensor is not potted and the low dielectric strength of helium is not adequate to prevent arc-over in the sensor. Sealing the high-voltage areas of the sensor from the helium environment is being considered as an alternative to running the test in a vacuum.

Acquisition gate logic. The *Mariner C* attitude-control mechanization included the use of brightness signals from the star tracker to aid in the acquisition of Canopus during the roll-search operation. A roll-search signal was applied whenever the brightness of an object, seen by the tracker, was outside the nominal range of ¼ to 8 times Canopus. The number of acquirable objects is thus reduced, requiring fewer roll override commands.

A flaw in this automatic system was discovered on *Mariner IV*. Particles from the spacecraft, tumbling through the tracker field of view, caused momentary flashes of sufficient brightness to violate the high gate logic and initiate a roll search, disacquiring Canopus. The problem was solved by transmitting DC-15, which removed the brightness gate logic. An unfortunate by-product was that automatic gyro turn-on for an unexpected loss of acquisition was also inhibited by DC-15. If the spacecraft were to lose Sun acquisition, reacquisition would be seriously compromised, possibly jeopardizing the power system, if a command to rescind DC-15 were late.

A high gate is required to prevent sustained acquisitions on the Earth; if the Canopus sensor locks on the Earth longer than 15 min, permanent degradation may result. The high gate also reduces the number of roll-override commands necessary to accomplish rapid Canopus acquisition. The standard trajectories selected for 1967 are unique, in that the cone angle of the Earth is never less than 110 deg. The field of view of the Canopus sensor extends from 74 to 106 deg, precluding acquisition of the Earth and eliminating the requirement for a high gate. The high gate will be removed from the Canopus sensor for the Venus 1967 mission.

Other modifications. The Canopus sensor mounting location has been changed for the mission. This requires that the phasing of the roll position signal be inverted and that the mounting surface be machined parallel to the optical axis.

The cone-angle program of the sensor must be modified to follow the Canopus cone angle for this mission. This is easily accomplished in the sensor by inverting the polarity of the cone-angle power supply from the *Mariner C* design. Fig. 6 shows the alignment of the nominal field-of-view as a function of time and the extremes of Canopus cone angle which must be handled.

d. Earth sensor. *Mariner C* experience shows that a backup for aid in identifying the star Canopus is not necessary. Therefore, the Earth detector which was used in 1964 for this purpose is not required for the *Mariner* Venus 67 mission.

However, with slight modification, the Earth detector will provide a slightly degraded roll reference (the Earth) for performance of a midcourse maneuver in case of the failure of the Canopus tracker. The Earth detector to be used for the Venus 1967 mission will be called the "Earth

UNCLASSIFIED

UNCLASSIFIED

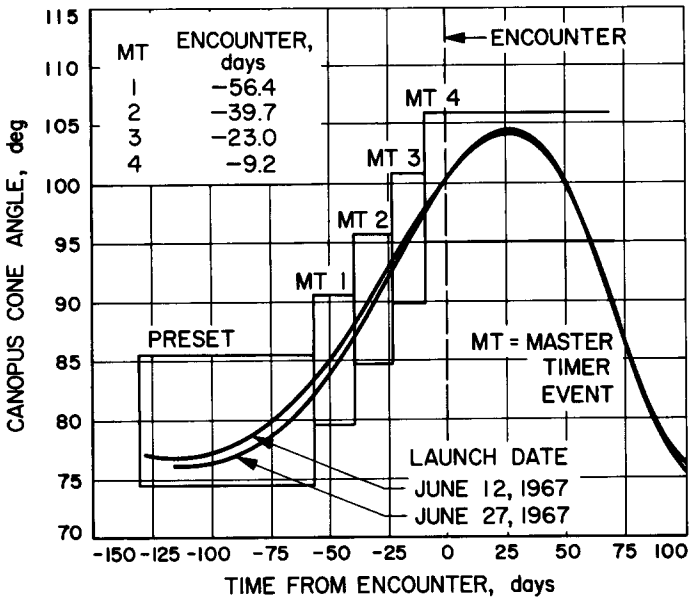

Fig. 6. Canopus cone angle and Canopus sensor field of view versus time

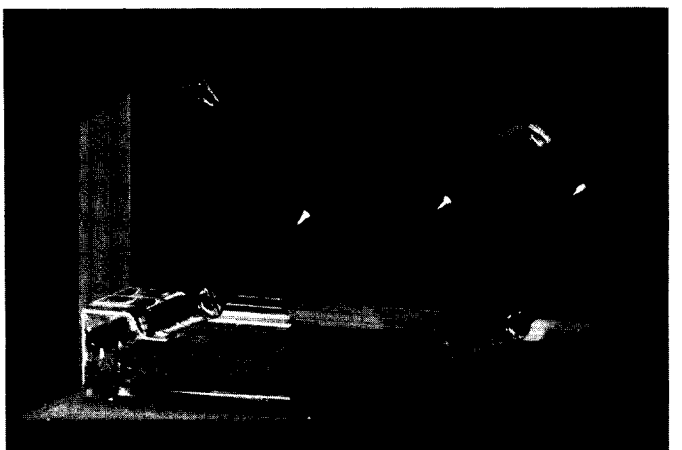

Fig. 7. The *Mariner* C Earth detector

sensor." Fig. 7 shows the Earth detector as used on *Mariner C* mission.

Earth sensor performance. The required modifications to the Earth detector will include redesign of all baffles to provide the proper fields of view. The clock-angle field of view will be 3.0 deg and the cone-angle field of view will be 50 deg. These angles are symmetrical about the Earth sensor's optical axis. The pointing angle of the device, with respect to spacecraft coordinates, will be 132 deg cone and 270 deg clock angle.

The absolute pointing accuracy of the sensor is equal to its clock-angle field of view (3 deg) plus its mounting accuracy. However, by ground command control of the spacecraft roll position and utilization of the information from the Earth sensor, the Earth-pointing accuracy can be greatly improved.

The range of operation is limited by the intensity threshold of the cadmium sulfide photoconductor used in the Earth sensor. This should provide a usable signal until a maximum of 20 days from injection.

Lunar interference should provide no problems, since the intensity of the Moon is below the sensor threshold beyond four days from injection. Prior to four days, the Earth/Moon intensity ratio is greater than 45 for all trajectory cases, and can easily be identified.

System operation of the Earth sensor. Use of the Earth detector would be made only in case of a complete failure of the Canopus tracker. After a tracker failure, the Canopus tracker would be turned off, the spacecraft placed in inertial mode, and a roll search initiated. The Earth detector would then provide an output, proportional to the Earth intensity, while the Earth was within the 3-deg field-of-view. At a roll rate of 0.2 deg/sec the Earth would remain in the Earth detector's field of view for approximately 15 sec. This means the Earth would roll through the 3-deg field-of-view, necessitating stopping the spacecraft and commanding reverse 2.25-deg roll steps until the Earth was within the proper field of view. By utilizing these manual means of control, the pointing accuracy to the Earth can be determined to better than ± 1.0 deg.

e. Terminator sensor. The *Mariner* Venus 67 mission has as its primary scientific experiment an S-band occultation experiment. One of the requirements of this experiment is an antenna-pointing-angle change (APAC) at midoccultation.

The terminator sensor will provide a signal to change the antenna pointing angle at the correct time. The sensor will sense the Venus terminator as the spacecraft passes through the occultation region. It will provide an electrical signal to the pyrotechnic package that will allow the antenna to move to a preset stop.

Sensor description and operation. The terminator sensor will be a *Mariner C* narrow angle Mars gate, shown in Fig. 8. Since the intensity of Venus is many orders of

UNCLASSIFIED

UNCLASSIFIED

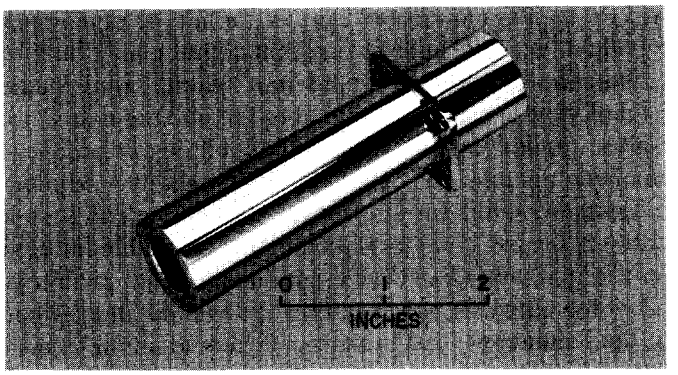

Fig. 8. *Mariner* C narrow angle Mars gate

magnitude greater than that of Mars, the intensity threshold of the sensor must be raised. This can be accomplished by changing the value of two resistors in the electronics module. Also under consideration is removal of the lens, since the cadmium sulfide detector is sensitive enough without optics.

The field of view of the sensor is 1.5 × 2.5 deg, with very good straylight rejection. The terminator sensor is cylindrically shaped, 4 in. long by 1 in. in diameter, with a mounting flange 1 in. from the back end. It weighs 0.16 lb, and nominally consumes 20 mw of power.

System operation. Fig. 9 shows the approximate encounter geometry relative to the terminator sensor. The pointing angle of the sensor will be chosen to provide a signal as close to the midoccultation point as possible. The angle must be chosen as a compromise between all possible trajectories and launch dates.

Since the light-scattering effect of the Venus atmosphere will tend to trigger the sensor early, the sensor must be mechanically biased toward the planet's center. The amount of bias will depend on studies now under way on the intensity profile of Venus.

f. Planet sensor. A planet sensor will be utilized for on-board initiation of the encounter sequence. The design

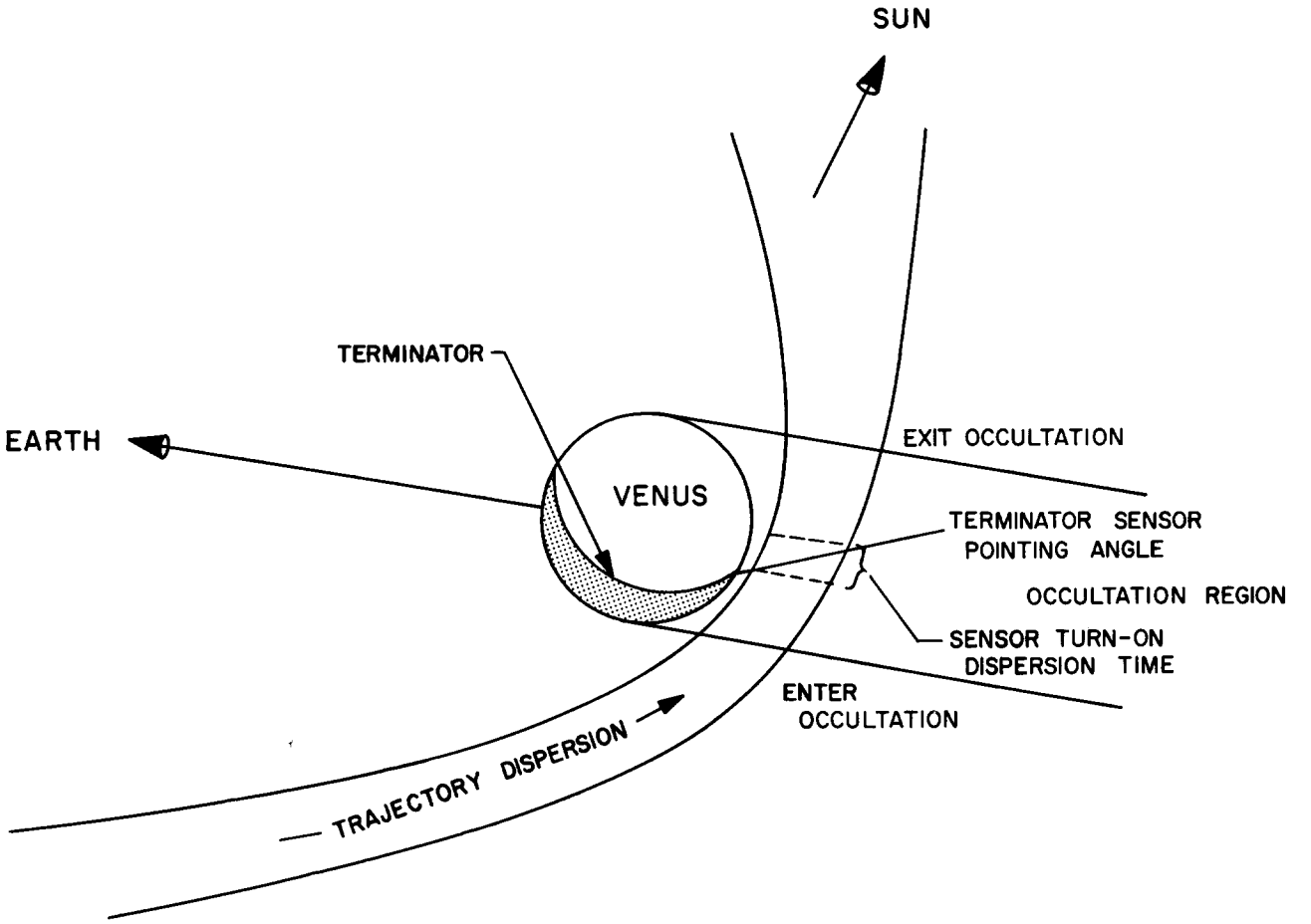

Fig. 9. Approximate encounter geometry relative to the terminator sensor

UNCLASSIFIED

UNCLASSIFIED

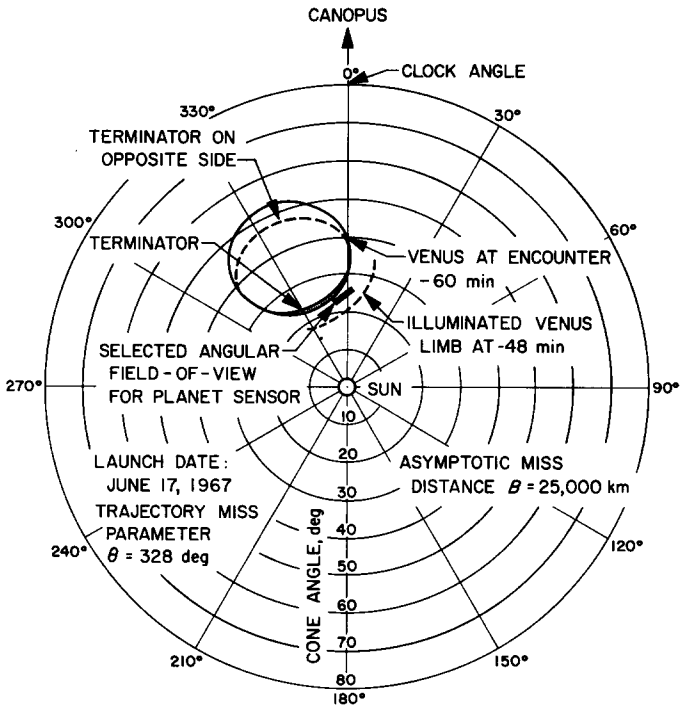

Fig. 10. Planet sensor field of view graphically superimposed, 2 min before activation (as seen from spacecraft)

center for the sensor output signal gate has been selected as encounter minus 1 hr. This is based on requirements of the ultraviolet photometer (high rate), tape recorder capacity, and dual-frequency radio propagation experiment, with allowance for the dispersions in sensor output timing accuracy. Backup to the planet sensor is provided by a ground-commanded initiation of a timer, 6 hr before encounter.

The planet sensor will function as a visual wavelength detector (cadmium sulfide) with a fixed field of view and will detect the illuminated limb of the planet as it enters this field. When a sufficient amount of the planet limb to exceed the detector threshold has entered the selected field of view, a gating signal will be fed into the data automation system. One of the more difficult design problems has been the selection of a field of view that would minimize timing errors for all planned trajectories and launch dates. A second problem is selection of a suitable location on the spacecraft that will minimize straylight problems, allow for adequate shading from the Sun (23 deg off one of the sensor axes) and provide sufficient room for mounting and changes in pointing angle if planned trajectories undergo further change.

Status. A field of view has been selected, and preliminary design of the optical system has begun. Fig. 10 depicts the selected sensor field of view and the location of Venus at 60 min before encounter for a particular launch date and trajectory.

The field of view selected provides a gating signal 60 $\pm$12 min (relative to encounter) for all combinations of trajectory dispersions and launch dates. This time dispersion was first determined by graphic iterations and then computer checked. The field of view selection also gave the minimum time dispersion relative to enter occultation, a secondary consideration.

Two probable spacecraft locations are being considered: (1) next to the Canopus tracker, and (2) on a spar supporting a solar panel opposite Bay I. The first location is currently being analyzed in detail.

A group of 100 detector cells has been received for testing, and a 33-cell test bed is being built for further environmental testing and selection. An optical system is in preliminary design.

References

1. "Attitude Control and Midcourse Guidance," *SPS 37-21*, Vol. II, pp. 34 to 54, May 31, 1963 (Confidential); "Magnetic Shielding for Canopus Tracker," *SPS 37-29*, Vol. II, pp. 25 to 37, September 30, 1964 (Confidential); "Test Results on the Effects of Ionizing Radiation on the *Mariner* C Canopus Sensor," *SPS 37-36*, Vol. II, pp. 3 to 9, November 30, 1965 (Confidential); "Proceedings of the XVI International Astronautical Congress," Athens, Greece, September 1965.

UNCLASSIFIED

UNCLASSIFIED

II. *Mariner* Mars 1969 Project

A. Introduction

The *Mariner* Mars 1969 Project was initiated in late December 1965 and formally tasked on February 1, 1966. The primary objective is to conduct two Mars flyby missions in 1969 to make exploratory investigations of the planet which will set the basis for future experiments—particularly those relevant to the search for extraterrestrial life. The secondary objective is to develop the technology needed for succeeding Mars missions.

The spacecraft design will be based on the configuration of the successful *Mariner IV* spacecraft, modified to meet the new needs of the 1969 mission objectives and to enhance mission reliability.

The launch vehicle will be the *Atlas/Centaur* SLV-3C. This vehicle, developed under contract for and direction by Lewis Research Center by General Dynamics/Convair, has a single- or double-burn upper-stage capability and a considerable performance increase over the *Atlas/Agena D* used in the *Mariner IV*.

Mariner Mars 1969 missions will be supported by the Eastern Test Range launch facilities at Cape Kennedy, the tracking and data facilities of the Deep Space Network, and other NASA facilities.

Activity on the Project during the period has been largely preparatory and preliminary. The Project has been staffed and quartered; the System Design effort is under way; and mission and interface studies are in process. Payload selection by NASA Headquarters is expected during the next period. Payload studies have begun, and preparations are under way for procurements for a number of spacecraft subsystems.

B. Systems

1. Mission Analysis

Both Type I and Type II transfer trajectories have been studied for the 1969 opportunity. Although it is possible to select an adequate Type II launch period for injection energies slightly smaller than those used for the Mars 1964 mission, these Type II transits have very long flight times and incompatible science aiming regions at Mars. The more advantageous Type II transits require much higher injection energies (25-30 km^2/sec^2) and must utilize early launch dates in November and December of 1968. However, as a result of significant effects upon schedule and also certain remaining undesirable features of Type II trajectories and their effect upon spacecraft design, the

CONFIDENTIAL UNCLASSIFIED

UNCLASSIFIED

decision was made to consider only Type I trajectories for the 1969 mission.

The Type I trajectories in 1969 exhibit large negative declinations of the departure geocentric asymptote. This geometrical condition places certain constraints upon the near-Earth launch geometry and thereby prevents the trajectory designer from centering the launch period in the minimum injection energy region. By utilizing the extra performance which can be achieved by launching a spacecraft of modest weight (700 to 800 lb) with the *Atlas/Centaur* SLV-3C, it is possible to use the southeast direct-ascent mode of launch from about early March through mid-April of 1969. It is possible to extend this launch period, if desired, by launching in February with a northeast parking-orbit profile. In fact, it is possible to utilize the two-burn mode from February until about mid-April, if desired. The currently preferred Type I arrival date period is between mid-July and early September of 1969. Regardless of whether the one-burn or two-burn mode of launch is selected for the mission, injection energy requirements are much higher than were previously required for the 1964 opportunity, thus preventing a dramatic increase in spacecraft weight. Fortunately, only a small increase is needed over that used in 1964 (570 lb).

Current plans and schedules have been adjusted to reflect an earliest possible launch date of February 1, 1969. However, as the early February trajectories are not as attractive as those launched after mid-to-late February and, in addition, as the somewhat less desirable northeast two-burn launch mode would have to be used during most of February, studies are currently in progress to assess how much value is realized by the extra amount of launch period which would be made available. Further analysis and evaluation of many tradeoffs is necessary before a final decision will be possible regarding the exact opening date of the Type I launch period.

C. Guidance and Control

1. Spacecraft Power

a. Introduction. In keeping with the *Mariner* Mars 1969 design philosophy, the power subsystem will be based upon a minimum departure from the *Mariner C* design. Most of the modifications will be made to the power-conditioning equipment in order to meet the new mission requirements and improve reliability. The solar panels and battery will be essentially the same as *Mariner C* equipment.

b. Redesign study. An examination of the mission and system requirements has led to a number of specific design-change recommendations discussed below.

In the new subsystem design the main regulator would be capable of supplying all loads, including the maneuver loads. The maneuver regulator then becomes a standby regulator, to be used only in the event of the failure of the main regulator. This will provide for a higher over-all efficiency due to reduced fixed losses in the regulators. The effects of turn-on transients of maneuver loads must be determined.

Redesign of the booster-regulator, to provide for a higher power-output capacity, greater efficiency, simplicity, reliability, and lower weight, has been studied and some tests have been performed. The output power will be increased from 150 to 170–200 w; output voltage may be increased to 85% at full load; and parts count would be reduced by the new design.

The main 2.4 kHz inverter (4A15) is expected to be redesigned to provide higher output capability and efficiency. An output power of 150 w as compared to approximately 100 w for the *Mariner C* design appears to be required. The efficiency can be increased to 90% as opposed to 86% for *Mariner C*. The recommended design incorporates a driver stage, using a series preregulator with a temperature coefficient which will allow the free-running output frequency to be maintained within $\pm 1\%$. This method serves as a backup frequency reference and eliminates the need for a separate oscillator. Efficiency is increased by using faster switching power transistor (2N3846), improved switching techniques, and improved synchronization. A minor change could be included which could improve the voltage telemetry accuracy. For *Mariner C*, the power transformer induced voltage was sensed by an auxiliary winding. This method does not account for transformer regulation losses. A more accurate method would be to use a small voltage-sensing transformer connected directly across the power transformer secondary winding.

The maneuver inverter (4A16) does not need to provide as much power as the main inverter and, therefore, may

UNCLASSIFIED

UNCLASSIFIED

be redesigned so that the fixed losses are lower and the efficiency is higher at the normal load. The inverter could be made smaller, simpler, and more reliable. Synchronization could be obtained from the output of the main inverter.

For the *Mariner* Mars 1969 spacecraft, the power synchronization is expected to contain the precision frequency reference for the spacecraft. This reference was in the CC&S subsystem for *Mariner C*. A crystal-controlled oscillator of either 38.4 or 307.2 kHz will be used. Integrated circuit flip-flops will be used to obtain the 2.4-kHz and the 400-Hz 3-phase signal. The method of synchronizing inverters will be changed to eliminate phase jitter. The main inverter will free run at 2.4 kHz $\pm 1\%$, eliminating the need for a backup oscillator in the synchronizer. The use of redundant precision oscillators is being considered. Several precision oscillator types are being investigated for suitability, and synchronizer circuitry is being breadboarded.

The battery charger (4A13) is being redesigned to reduce standby losses to 2 w as compared to 12 to 20 w for the *Mariner C* design. The battery voltage telemetry monitor will be modified to prevent trickle charging of the battery. A circuit has been designed and is undergoing testing.

A complete redesign of the power distribution subassembly will be necessary to meet new mission requirements. The present design can be simplified to some extent to improve reliability. The design will require a list of commands, responses, and signal input types (i.e., isolated switch, relay contact, or saturated transistor).

Modification to the 1-phase and 3-phase 400-Hz inverters will consist of minor changes in the design of the power transformers to accommodate the expected higher booster bus voltage.

c. Solar panels. A study was conducted to determine the effect of solar flare degradation on the performance of a *Mariner C* type of solar array. The results of this analysis indicate that a 27% degradation due to one solar flare is to be expected for a 1969 mission with a duration of up to 12 mo.

A study of the tradeoffs in using thicker coverglasses to prevent damage to solar cells from solar flare proton activity has been made. The study shows that if the thickness of the present coverglass is increased from 6 to 20 mils, the degradation would be reduced to 22%. This reduction would increase the weight of the solar array by 12%. The thickness of solar cell coverglasses would have to be increased to 60 mils to realize a substantial reduction in damage. This increase would result in a prohibitive increase in solar panel weight.

UNCLASSIFIED

UNCLASSIFIED

III. *Voyager* Project

A. Introduction

1. Objectives

The primary objective of the *Voyager* Program is to carry out scientific investigations of the solar system by instrumented, unmanned spacecraft which will fly by, orbit, and/or land on the planets. Emphasis will be placed on acquisition of scientific information relevant to the origin and evolution of the solar system, the origin, evolution, and nature of life, and the application of this information to an understanding of terrestrial life. The primary objective of the *Voyager* mission to Mars, beginning in 1973, is to obtain information relative to the existence and nature of extraterrestrial life, the atmospheric, surface, and body characteristics of Mars, and the planetary environment by performing unmanned experiments on the surface of, and in orbit about, the planet. A secondary objective is to further our knowledge of the interplanetary medium between the planets Earth and Mars by obtaining scientific and engineering measurements while the spacecraft is in transit.

2. Project Plan

All *Voyager* missions will be conducted as events of an integrated program in which each individual flight forms a part of a logical sequence in an over-all technical plan of both lander and orbital operations. The *Voyager* design will provide for the carrying of large scientific payloads to the planet, the telemetering of a high volume of data back to Earth, and long useful lifetimes in orbit about the planet and/or on the planetary surface. Hardware will be designed to accommodate a variety of spacecraft and/or capsule science payloads, mission profiles, and trajectories. Particular emphasis will be given to simple and conservative design, redundancy wherever appropriate, and a comprehensive program of component, subsystem, and system testing.

Over-all direction and evaluation of the *Voyager* Project is the responsibility of the Office of Space Science and Applications (OSSA) of the National Aeronautics and Space Administration (NASA). Management of the *Voyager* Project and implementation of selected systems is the responsibility of the Jet Propulsion Laboratory (JPL) of the California Institute of Technology (CIT).

3. Technical Description

Two *Voyager* planetary vehicles are to be designed, constructed, and tested for launch on a single *Saturn* V during the 1973 Mars opportunity. Attention is also being given to requirements imposed on such vehicles by launches subsequent to 1973, such as a similar mission planned for 1975. Each planetary vehicle is to consist of a flight spacecraft and a flight capsule, with science experiments conducted in 1973 both from the orbiter and on the planetary surface. The flight spacecraft with its several hundred pounds of science payload will weigh approximately 2500 lb, its retropropulsion subsystem may additionally weigh up to 15,000 lb, and the flight capsule

UNCLASSIFIED

UNCLASSIFIED

will weigh about 3000 lb, or less. The flight spacecraft will be a fully attitude-stabilized device utilizing celestial references for the cruise phase, and will be capable of providing velocity increments for midcourse trajectory corrections and for Mars orbit attainment by both the flight spacecraft and flight capsule. Onboard sequencing and logic will be provided, as well as ground command capability. The flight spacecraft will supply its own power from solar energy or from internal sources and will be capable of maintaining radio communications with Earth. In addition, the flight spacecraft will be thermally integrated and stabilized and will monitor various phenomena near Mars and during transit, and telemeter this information back to Earth; it will also monitor and telemeter data pertaining to spacecraft operation. The flight spacecraft will also provide the flight capsule with services such as power, timing and sequencing, telemetry, and command during the transit portion of the missions and may also serve as a communications relay. The sterilized flight capsule will be designed for separation from the flight spacecraft in orbit, for attaining a Mars impact trajectory, for entry into the Mars atmosphere, descent to the surface, and impact survival, and for surface lifetimes of two days in 1973 and later goals of as much as 6 mo. The flight capsule will contain the power, guidance, control, communications, and data handling systems necessary to complete its mission.

No deep space-flight tests of the flight spacecraft are planned, and compensation will be made by additional ground tests conducted to the extent possible. The test program for the flight capsule, which is planned to include Earth-entry flight tests will investigate entry dynamics.

B. Project Engineering

1. Proton Irradiation of Mariner C Canopus Tracker, Data Encoder, MOSFETS,[1] Photons Switches, and Integrated Amplifiers

a. Introduction. A proton irradiation testing program to obtain data for the *Voyager* spacecraft was initiated with the following objectives: (1) to determine the feasibility of using a high-energy proton beam produced by an accelerator to simulate proton radiation fields found both in the Earth's Van Allen belts and in the emission from solar flares and (2) to examine the response of two typical *Mariner C* subsystems to this simulated environment, choosing subsystems whose response to electron irradiation was already known (*SPS 37-34*, Vol. II, p. 2, July 31, 1965). Testing is being done on *Mariner C* subsystems, as the hardware for *Voyager* has not yet been selected.

According to our calculations, using the Vette AP1 model for Van Allen belt protons, the maximum proton flux for a *Mariner* Venus 67 trajectory is 1.3×10^4 protons cm^{-2} sec^{-1} ($E > 34$ Mev). It is expected that *Voyager* trajectories will encounter similar fluxes. Consequently the testing program should bracket this flux in addition to covering the solar flare flux spectrum.

The next maxima in sunspot activity is expected to occur in 1969. Past observations have shown that solar flare events producing extremely high energy protons are more likely to occur one or two years before and after the maxima. Consequently, spacecraft in interplanetary space in 1967 through 1973 can expect an enhanced probability of encountering solar flare protons. The maximum solar flare proton flux observed at the Earth during the preceding solar cycle maximum was 1.8×10^4 protons cm^{-2} sec^{-1} ($E > 30$ Mev) for the July 16, 1959 flare (Ref. 1). However, this number is a calculated value based on data taken from Earth-based laboratories. The data and its interpretation are subject to quite large uncertainties. There is still additional problem in using the Earth-based data to extrapolate flux values to the relatively field-free region in interplanetary space. Finally, we are almost completely ignorant of how to predict solar flare activity and the associated solar proton fluxes for an upcoming solar cycle. The solar proton fluxes during the next cycle could be orders of magnitude higher or lower than those of the preceding cycle. Therefore, it would be prudent to use a large safety factor when assessing the capability of spacecraft hardware to function in a solar proton field.

The synchrocyclotron at Harvard University was chosen as the proton source because it could produce the energies and flux rates needed for simulation of both radiation fields, namely, 20 to 137 Mev and 10^4 to 10^7 protons cm^{-2} sec^{-1} over the subsystem surfaces. 20 Mev is the minimum energy needed to penetrate into the subsystem electronics.

b. Test setup and calibration. The test setup used at the Harvard synchrocyclotron site is diagrammed in Fig. 1. The machine produces 160-Mev protons in a beam which is focussed on the lead-scatterer. The protons undergo multiple scattering collisions in the lead-scatterer

[1]Metal-oxide-silicon field effect transistors.

UNCLASSIFIED

UNCLASSIFIED
CONFIDENTIAL

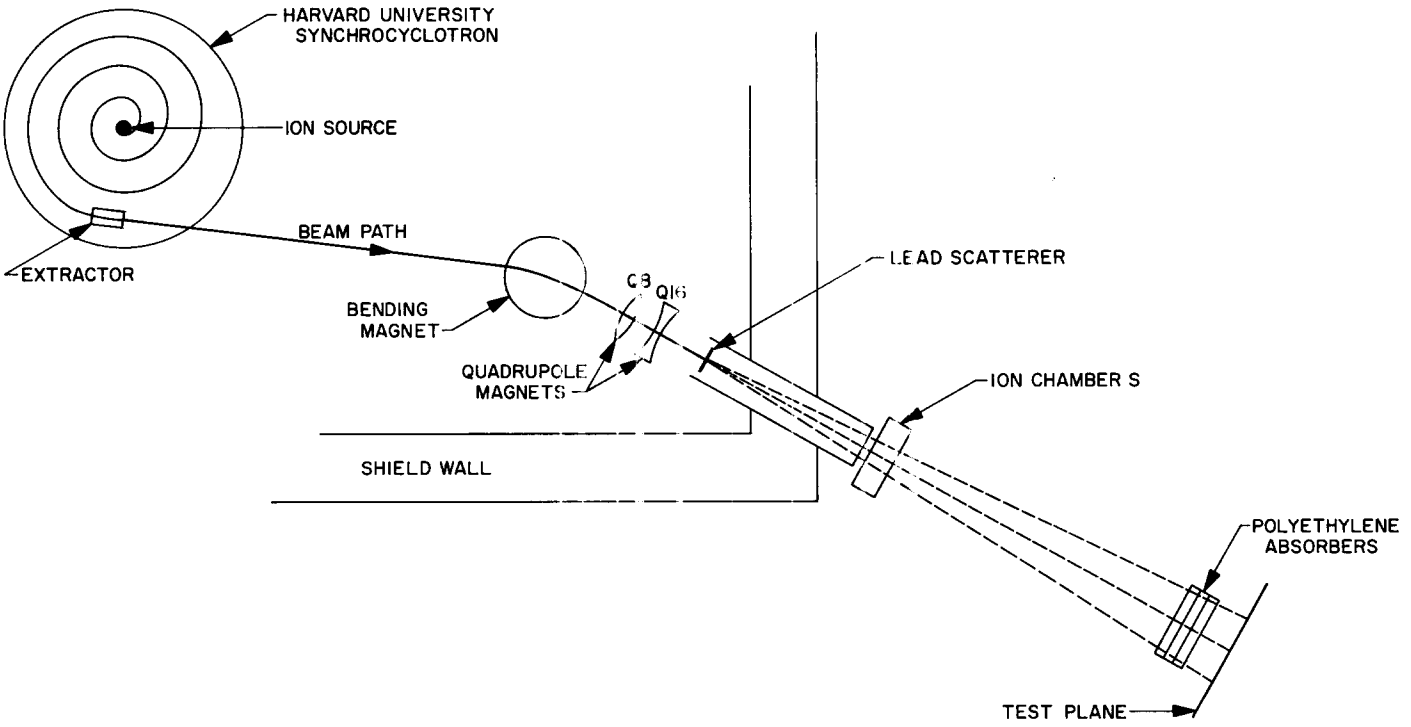

Fig. 1. Synchrocyclotron facility

and emerge with reduced energy but with sufficient angular divergence to produce a circular cross-section of 18-in. D at the test plane. The ion chamber S is used to monitor beam intensity. Polyethylene absorbers may be placed in front of the test plane to reduce beam energy. Without the absorbers, beam energy at the test plane is 137 Mev.

The subsystems were connected by 50-ft cables to the operational support equipment located in the accelerator control room.

Having focussed the beam on the scatterer, the beam intensity profile was mapped at the test plane by means of a small defined volume ionization chamber (DVIC). Results of the horizontal and vertical mapping traverses are shown in Figs. 2 and 3. Fig. 4 shows contour curves of this flux distribution at the test plane superimposed on a scale diagram of the data encoder subchassis and circuit boards which held the test electronic components as they were positioned in the beam. The Canopus tracker would lie entirely within the 90% contour.

Absolute beam flux calibration was achieved by placing a Faraday cup and lead collimator at the beam center in the test plane. It was found that the flux at the beam center in the test plane could accurately and repeatedly be related to the current collected in ionization chamber S. This calibration procedure allowed subsequent bombardment of objects lying in the test plane without the necessity of also mounting a Faraday cup nearby.

c. Test procedure. The test item, centered in the test plane, was first irradiated at 137 Mev with low fluxes for a time sufficient to assess performance while operating in the beam. Fluxes were gradually increased to determine a possible failure threshold flux, with frequent beam interruptions to search for permanent damage effects and perform a thorough system checkout. If no malfunctions occurred with maximum available flux from the cyclotron, the item was irradiated to an integrated flux of about 4×10^{10} protons cm^{-2}. At this point the beam energy was reduced and the procedure repeated. The circuit boards containing the electronic components were, however, removed from the beam at an integrated flux of 10^{10} protons cm^{-2}, since they were not instrumented for "beam on" monitoring.

This procedure was augmented during Canopus tracker testing by shielding various areas of the tracker from the beam in order to pinpoint trouble areas.

d. Results

Data encoder. The data encoder received integrated fluxes of 4.4×10^{10} protons cm^{-2} at 137 Mev, 4.1×10^{10}

CONFIDENTIAL
UNCLASSIFIED

UNCLASSIFIED

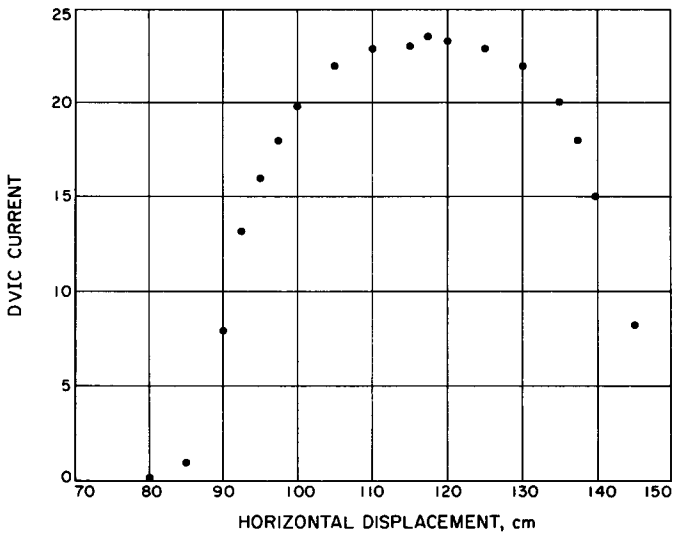

Fig. 2. Horizontal beam profile in test plane

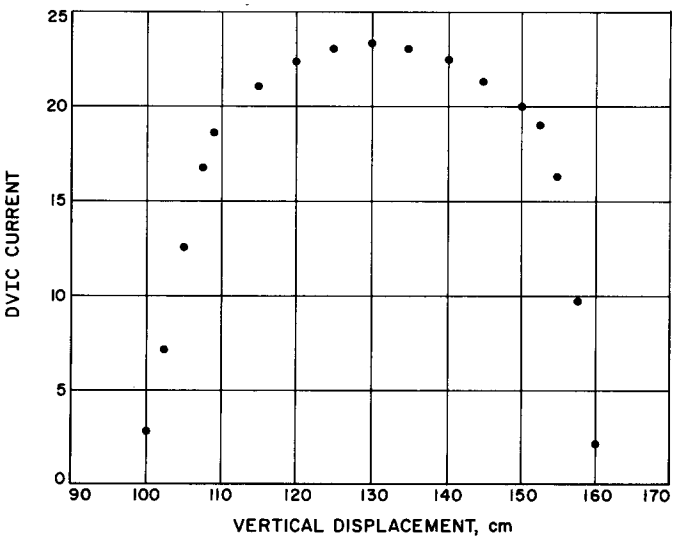

Fig. 3. Vertical beam profile in test plane

protons cm^{-2} at 99 Mev, 4.1 × 10^{10} protons cm^{-2} at 59 Mev, and 4.3 × 10^{10} protons cm^{-2} at 33 Mev for a total integrated flux of 1.7 × 10^{11} protons cm^{-2}. This is equivalent to a surface dose of 2.2 × 10^{4} rad (aluminum). The highest flux rate used was 1.0 × 10^{7} protons cm^{-2} sec^{-1}.

The resultant effects on the data encoder were negligible. If an equivalent radiation was encountered in flight, it would be difficult to determine whether the changes were due to radiation or to the expected variations due to aging and normal sensor value shifts. No deck resets or skips, event counter changes, out-of-lock indications, or

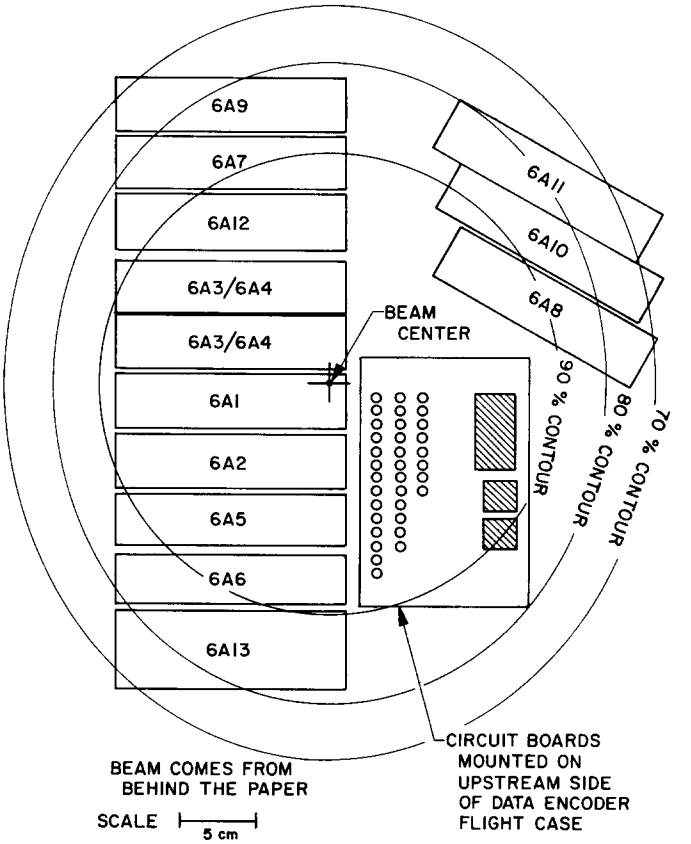

Fig. 4. Constant flux contours superimposed on data encoder placement in the test plane

other transitory behavior were observed. As far as permanent damage is concerned, only three channels of the 49 excited changed in value; and those changed by only one data number. This was caused by slight changes in the analog-to-digital converter quantization levels. On the basis of this test, we conclude that the data encoder can operate in space during a maximum solar cycle without observable radiation-induced malfunction.

MOSFETS, photon switches, integrated circuits. Four circuit boards containing photon switches, integrated circuits, and MOSFETS were irradiated simultaneously with the data encoder, each board receiving one proton energy and a flux of 10^{10} protons cm^{-2}. Permanent parameter changes, on the average, were as follows for the MOSFETS[2]: (1) 40% increase in *ON* resistance, (2) 10% decrease in transconductance, (3) 10% increase in average leakage current, and (4) no change in breakdown or threshold voltages. There was a 3% decrease in bipolar transistor beta and a 10% increase in photon switch *ON*

[2]Ponder, J., IOM 3342-66-141, March 24, 1966.

UNCLASSIFIED

UNCLASSIFIED

resistance. No energy-dependent effects could be determined. There was no change in operating characteristics of the integrated circuits.

The units irradiated were:

(1) Raytheon FN 1034
(2) GME 2N3608
(3) TI TIX511
(4) Fairchild FI100
(5) Motorola MM2102
(6) Motorola MM2103
(7) PNP bipolar transistor 2N995
(8) NPN bipolar transistor 2N2369
(9) IBM developmental photon coupled switch with Ga as diode
(10) TI developmental photon coupled switch and Ga as diodes
(11) Fairchild 9040 integrated circuit flip-flop
(12) Fairchild 9041 integrated circuit gate
(13) TI SNX1503 integrated circuit gate

Canopus tracker. 95 irradiations of the tracker were carried out in the energy range 19.5 to 137 Mev. 76 irradiations were incident on the left cover surface for a total integrated flux of 2.1×10^{10} protons cm^{-2} and 19 irradiations were incident on the front surface for an additional integrated flux of 2.8×10^{9} protons cm^{-2}.

Fig. 5 shows the flux failure thresholds found when the tracker was irradiated with beam incidence on the left surface and on the front surface (end-on). It is apparent that if the protons have sufficient energy to reach the image dissector tube a flux of 6×10^{5} protons cm^{-2} sec^{-1} is sufficient to cause loss of roll control.

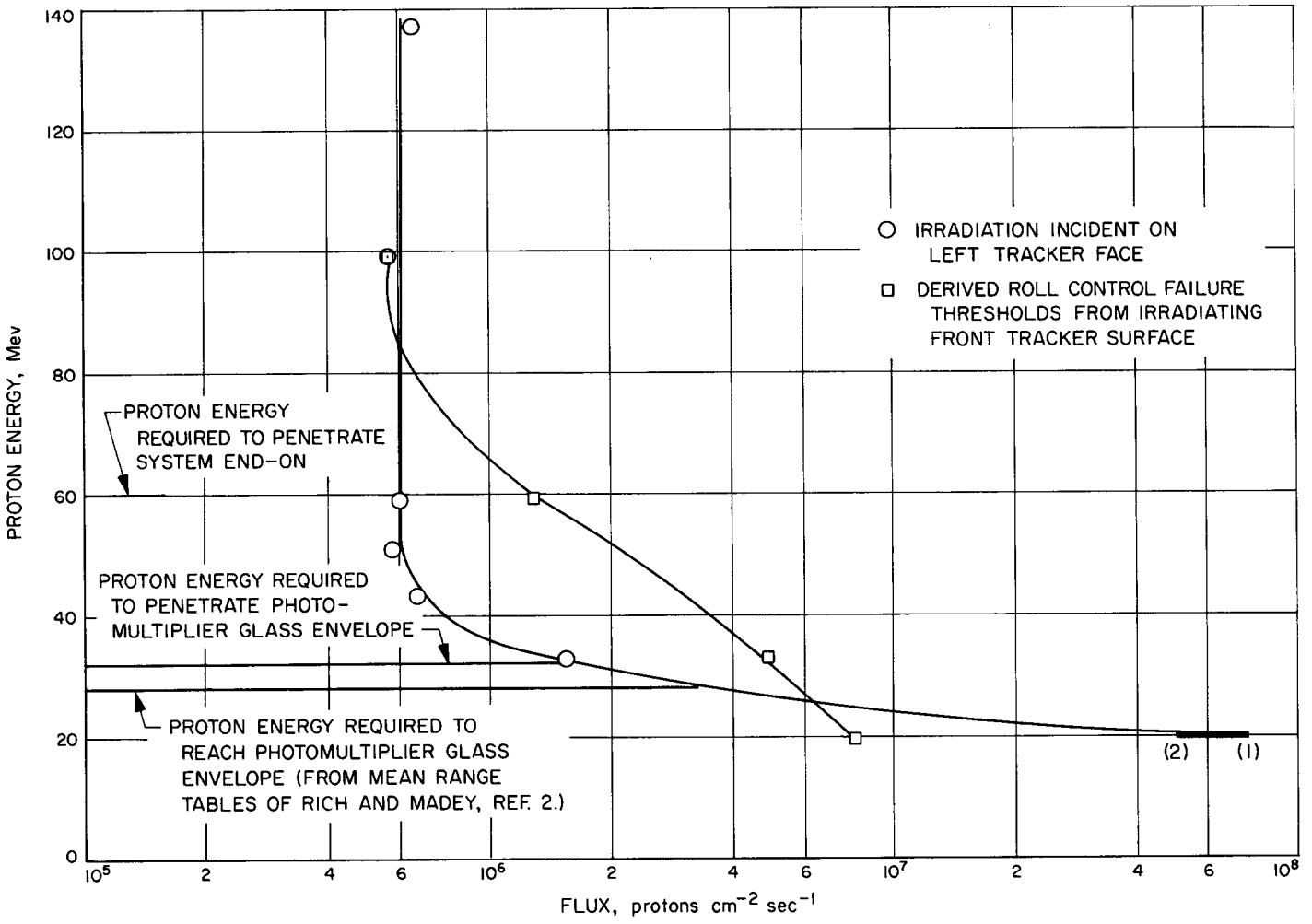

Fig. 5. Failure thresholds for Canopus tracker to lose roll control

UNCLASSIFIED

UNCLASSIFIED

Shielding various parts of the tracker from the beam indicated that the dynode area of the image dissector tube was the most radiation-sensitive portion of the tracker. The front lens element was also found to be quite sensitive to higher proton energy radiation. Tracker performance was degraded for about 12 hr after heavy radiation. We postulate that this is due to low-level radioactivity induced by the beam in the glass associated with the image dissector envelope and optics, as well as in the electron multiplier section.

e. Discussion. It is interesting to note that the Canopus tracker failed at a flux of 6×10^5 protons cm^{-2} sec^{-1} for $E > 40$ Mev and at 2×10^9 electrons cm^{-2} sec^{-1} for 2 Mev electrons (*SPS 37-34*, Vol. II, p. 2, July 31, 1965). The data encoder, on the other hand, did not fail in proton fluxes as high as 10^7 protons cm^{-2} sec^{-1}, but failed at 10^9 electrons cm^{-2} sec^{-1} for 2 Mev electrons. That is, the data encoder is more radiation-sensitive subsystem of the two in an electron field, but the tracker is the more sensitive in a proton flux. For the tracker the ratio of the electron flux failure threshold to the proton flux failure threshold is 3.3×10^3, but the ratio of the proton stopping power to electron stopping power is only about 10. Therefore, it is clear that the stopping power of the beam in the subsystem is not the main cause for the tracker failure in one or both of the radiation fields. It is, therefore, very dangerous to predict subsystem performance in a given type of radiation field, even when the performance is known in another type of field if the prediction is based on particle parameters derived from the stopping powers.

C. Engineering Mechanics

1. Variable Trimming Resistor Sterilization Test Program

a. Introduction. The primary objective of the electronic component sterilization test program recently initiated at JPL is to establish a sterilization parts list which tabulates the electronic component parts capable of withstanding several 36-hr periods of nonoperational storage at 145°C without significant degradation. A secondary objective is to use the test results of a 10,000-hr life test to compare vendor quality and to perform analysis of long-term failure modes. The parts to be tested are selected on the basis of anticipated usage and potential susceptibility to damage from heat sterilization. The results of the test performed on variable trimming resistors are presented here.

b. Test description. A total of 2,640 resistors (110 each for 24 codes) were ordered (Table 1). The manufacturers

Table 1. Test item description for sterilization test program

Code	Manufacturer	Part Number	Type	Resistance, ohms	Tolerance ± %	Maximum watts	Operating Temperature, °C	Maximum Temperature, °C	Dimensions, in.
1 2 3	Borg Electronics	2750-L	Wire wound	100 10K 30K	5	1.0	70	175	1.25 × 0.32 × 0.19
4 5 6	Borg Electronics	2900-L	Wire wound	100 10K 30K	5	1.0	70	175	0.5 × 0.5 × 0.187
7 8 9	Borg Electronics	2950-L	Metal film	500 10K 20K	10	1.0	70	175	0.5 × 0.5 × 0.187
10 11 12	Bourns, Inc.	224L-647-101 224L-647-103 224L-647-503	Wire wound	100 10K 50K	5	1.0	70	175	1.25 × 0.32 × 0.19
13 14 15	Bourns, Inc.	3280L-647-101 3280L-647-103 3280L-647-503	Wire wound	100 10K 50K	5	1.0	70	175	0.375 × 0.375 × 0.203
16 17 18	Dale Electronics	697	Wire wound	100 10K 30K	5	1.0	70	175	1 × 0.32 × 0.18
19 20 21	Dale Electronics	5050	Wire wound	100 10K 50K	5	1.0	70		0.5 × 0.5 × 0.19
23 24 25	Bourns, Inc.	3051L-647-203 3051L-647-104 3051L-647-504	Carbon	20K 100K 500K	20	0.20	70	150	1.25 × 0.32 × 0.19

UNCLASSIFIED

UNCLASSIFIED CONFIDENTIAL

were informed of the intended sterilization use and were required to burn-in each resistor for 250 hr at rated wattage and temperature prior to shipment. The units were forwarded to The Boeing Company, Huntsville, Alabama, where they were evaluated in accordance with JPL Contract 950790.

Each of the selected manufacturer's part types were divided into four groups:

Group A. No sterilization temperature cycling; rated power applied during life.

Group B. Three sterilization temperature cycles; rated power applied during life.

Group C. Six sterilization temperature cycles; rated power applied during life.

Group D. Six sterilization temperature cycles; no power applied during life (shelf life investigation).

Total resistance and voltage ratio of all samples were measured before and after sterilization temperature cycling and at specific periods during the 10,000-hr life test. Total resistance is the resistance of the entire element in a variable trimming resistor. Voltage ratio is a measure of the wiper with reference to one end of the resistor element. Voltage ratio setting is used to determine wiper drift and wiper contact resistance during life testing. In addition, resistance measurements were taken for calculating temperature coefficient before and after sterilization temperature cycling and also following the 10,000-hr life test. Upon completion of the 10,000-hr life test, Group D parts were removed from temperature storage and in conjunction with Group C, were subjected to an additional 250-hr life test at rated wattage and temperature. The purpose of testing Group D is to simulate conditions where equipment would be on an extended nonoperational mission and then turned on remotely at or near its destination. Group C is included as a comparison control group operating at rated power and temperature.

c. Test results. At the beginning and end of the test program, all samples were given a wiper noise test. Noise is any electric signal or disturbance which interferes with the desired electrical output. Equivalent noise resistance (ENR), expressed in ohms, is the effective resistance between the wiper and the resistance element, as the wiper traverses the element. In testing for equivalent noise resistance, a constant current is passed through the wiper circuit. The noise then appears as a random voltage which, when amplified, is audible, or visible on an oscilloscope. Noise, if any, usually occurs only during potentiometer adjustment; no noise should exist when the wiper is stationary. The initial noise test revealed 22 catastrophic failures of the Borg 2950—most of them due to the breaking of the bond between the lead wire and the metal-film element of the trimmer. The Bourns 3280 had 19 catastrophic failures during the final noise test. Analysis revealed that the plastic wiper gear had changed composition and was easily stripped by the drive screw. The number of sterilization cycles did not seem to critically affect the number of failures in any group. There were no significant differences between the 10,000-hr operational life and the 10,000-hr nonoperational storage test results.

Of the eight vendor part types tested, the following four are recommended for sterilized spacecraft use: Bourns 224L (Codes 10, 11 and 12), Bourns 3280L (Codes 13, 14 and 15), Dale 697 (Codes 16, 17, and 18), and Bourns 3051L (Codes 23, 24, and 25).

D. Guidance and Control

1. Spacecraft Power: Sterilizable Battery

a. Development of separators for sterilizable batteries. A program to develop a separator material for use in a Ag-Zn or Ag-Cd battery has been established. The work is being done by several companies which are under contract to JPL. One of the separator materials obtained under Contract 951015 with RAI Research Corp. is still being evaluated. The contracts at four companies — The Southwest Research Institute, Lockheed-Georgia Co., Martin-Marietta Corp., and High Energy Processing Corp. — to produce a uniform product using a procedure developed under the RAI Contract 951015 are in different levels of completion. Some of the materials produced have been delivered and are being evaluated. The Narmco Division, Whittaker Corp., has produced a film from poly-2,2′-(hexamethylene)-5,5′-bibenzimidazole, for which the values for resistivity and tensile strength in the initial testing were satisfactory.

Separator material from JPL Contract 951015. The Electric Storage Battery Co. and JPL are continuing to evaluate RAI-116 for uniformity and performance characteristics in Ag-Zn cells. Resistivity data, which have been used as a measure of film uniformity, have been obtained for 81

UNCLASSIFIED CONFIDENTIAL

UNCLASSIFIED

samples. The average value is 0.010 ohm-in^2 with a standard deviation of 0.006 ohm-in^2. No conclusions have been derived from electrical capacity measurements.

Separator materials from two of the four companies contracted to produce uniform RAI-116 are being evaluated. The data are not sufficient to provide conclusions.

JPL Contract 951091 with Narmco Division, Whittaker Corp. A number of films prepared from copolymers of diaminobenzidine and mixtures of sebacic and suberic acids have been cyanoethylated to varying degrees.

A film prepared from the highly cyanoethylated copolymer of suberic acid and diaminobenzidine had a sufficiently low resistivity value, and the continuation of this program will deal with modifications of film preparation with the intent of establishing the procedure necessary for the fabrication of large amounts of uniform material.

b. Research and development of the heat-sterilizable battery. The contract with the Electric Storage Battery Co., Yardley, Pa., is for a research and development program for sealed Ag-Zn and Ag-Cd cells capable of providing satisfactory electrical performance after heat sterilization in the uncharged condition and high-impact resistance after charging.

In the electrochemistry task the electrical conductivity studies of KOH and ZnO-KOH solutions have been completed. The data for both solutions of conductivity versus concentration at 10, 25, and 55°C have been corrected by new measurements of solution concentrations. Some rates of dissolution of ZnO powder in KOH have been measured at room temperature and at 125 and 145°C for conditions of stirred and unstirred solutions. The rate is dependent upon KOH concentrations for unstirred solutions. This dependence disappears for stirred solutions. The powder studies have been completed; the investigation of the dissolution rate with ZnO electrodes is under way.

The formation efficiencies of the electrodes as a function of formation rate are being measured to provide estimates for the charge and discharge schedules to be used in the design of cells with RAI separators. The graph of percent theoretical capacity versus hours of charge is reasonably linear for data before sterilization. These data will also be obtained after sterilization.

A study of components is being made to determine the cause for decreased capacity after sterilization. A series of experiments in which the different components of the cell had been sterilized before capacity tests led to the conclusions that the HgO in the Zn electrode and the polypropylene absorber caused decreases in capacity of the Ag electrode. One of the efforts to prevent the loss is the substitution of asbestos for polypropylene.

In the cell case task design changes have been made in the molded cases and covers. Studies continue on the terminal and case sealing problems, using the techniques of ultrasonic welding and adhesive sealing. Neither of these methods is adequate at present.

E. Telecommunications

1. A Spacecraft Engineering Data-Handling System Using Data-Compression Techniques

The objective of the engineering data-handling system (EDHS) is to reduce the bandwidth requirements and greatly increase the sampling frequency of engineering data channels. This system, or a permutation of it, is proposed for use on *Voyager*-type missions to increase information content of data gathered for engineering measurements.

During the conceptual design of the EDHS, spacecraft engineering measurements were divided into the following four categories:

(1) Mission-critical. The most critical measurements for which the high reliability requirement justifies the nonoptimization of bandwidth (using real-time commutation without data compression techniques).

(2) Operational. Critical measurements which are data compressed but which require an essentially real-time path to Earth for "quick look" monitoring and for operational decisions.

(3) Performance (high and low sampling frequency). Noncritical measurements requiring the information available from a zero-order-compressed data profile.

(4) Evaluation. Noncritical measurements requiring the information available from a data profile consisting of data compressed by some means other than zero-order comparison.

UNCLASSIFIED

UNCLASSIFIED

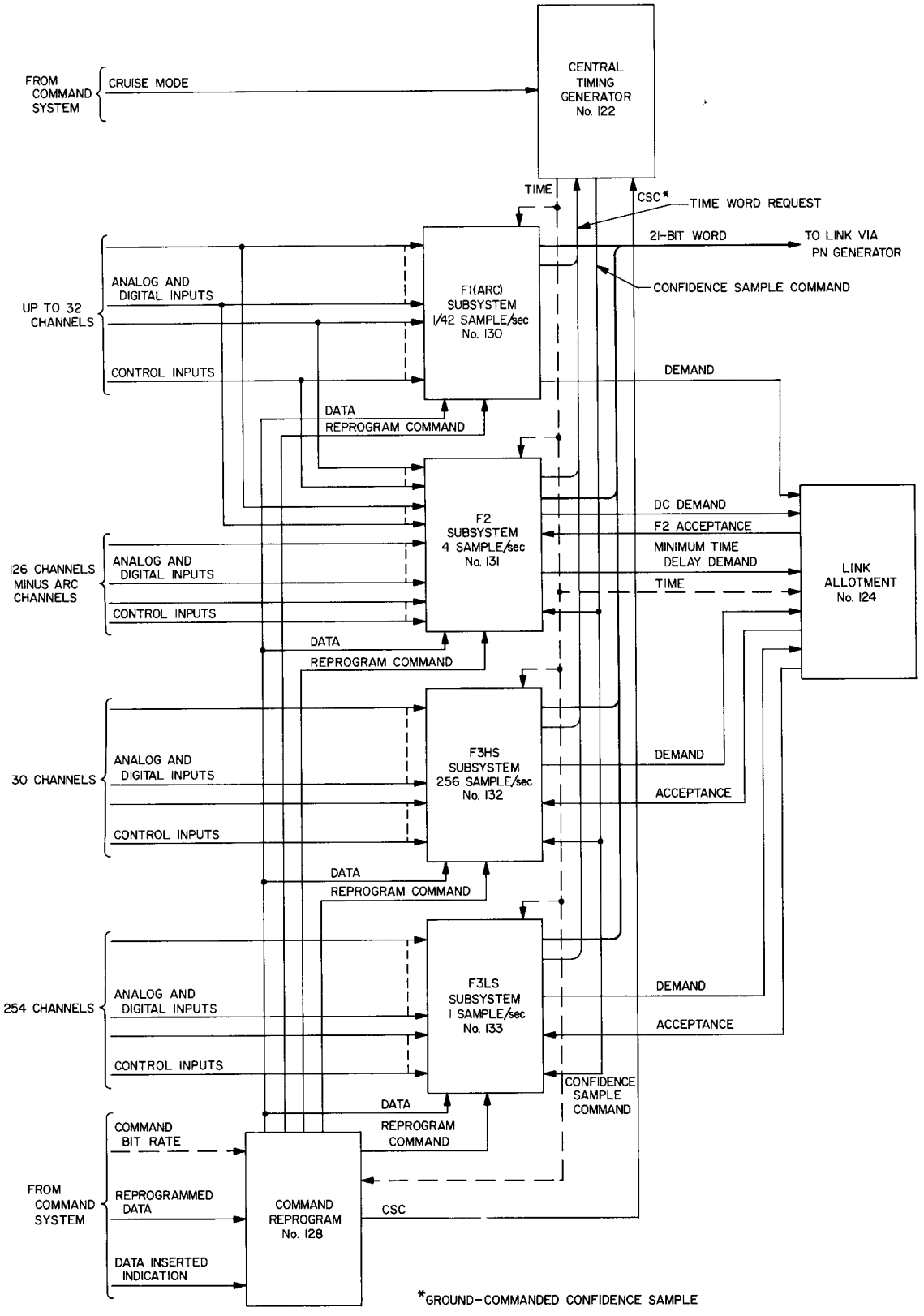

Fig. 6. EDHS block diagram

UNCLASSIFIED

UNCLASSIFIED

From the first three of these four measurement categories, four subsystems evolved:

(1) F1—later called the absolute rate commutator (ARC)—for mission-critical measurements

(2) F2 for operational measurements

(3) F3HS for high-speed performance measurements

(4) F3LS for low-speed performance measurements

The type of subsystem required for the fourth category (evaluation) falls outside of the scope of this effort. Therefore, no actual design was evolved.

A block diagram of the complete system as designed is shown in Fig. 6. Peripheral modules are also shown, such as the link allotment module (responsible for sequencing the data into the transmission link), the command reprogram module, and the central timing generator.

Each of the data compression subsystems (F2, F3HS, and F3LS) is provided with: (1) a user's control function to enable or disable each channel at the discretion of the user, (2) a confidence sampling path which will automatically and/or upon command allow samples to bypass the processor and be sent in real-time, and (3) a ground commanded reprogramming capability.

a. F1 subsystem. The F1 subsystem does not compress data; it consists of a real-time absolute rate commutator in which each user has two possible sampling rates and may switch inflight between the two (Fig. 7). The sampling rate of an individual channel equals the commutator scan rate times $1/2^n$ where $n = 0, 1, 2, 3, \ldots$ and each channel is programmed with two different values of n. This algorithm is realized by rejecting channel samples from all but the 2^nth scans.

b. F2 subsystem. F2 is a data compressive subsystem with 126 data channels and 2 time channels (Fig. 8) in which the significance detector is a zero-order comparator, the buffer input cutback scheme is the reduction of channel allotment of buffer volume, and a minimum time delay path is provided.

Zero-order comparator. In zero-order compression a comparison is made between the amplitude of the present sample and that of a reference sample. If the present sample value differs from the reference value by more than the aperture, the sample is significant; if the sample is accepted and thus sent, it also becomes the new reference sample. This comparison is called zero order because a constant amplitude waveform corresponds to the polynomial $(a_0 + a_1T + a_2T^2 + \cdots + a_nT^n)$ in which all coefficients except a_0 are equal to zero. Zero-order compression of a typical active waveform is shown in Fig. 9. This type of data compression should be used for data that changes amplitude infrequently, such as propulsion pressures, positions, temperatures, and digital measurements. This compression method requires a minimum of equipment.

Allotment-of-buffer-volume. During periods of considerable measurement activity, the buffer might tend to overflow; thus there must be a cutback in the amount of

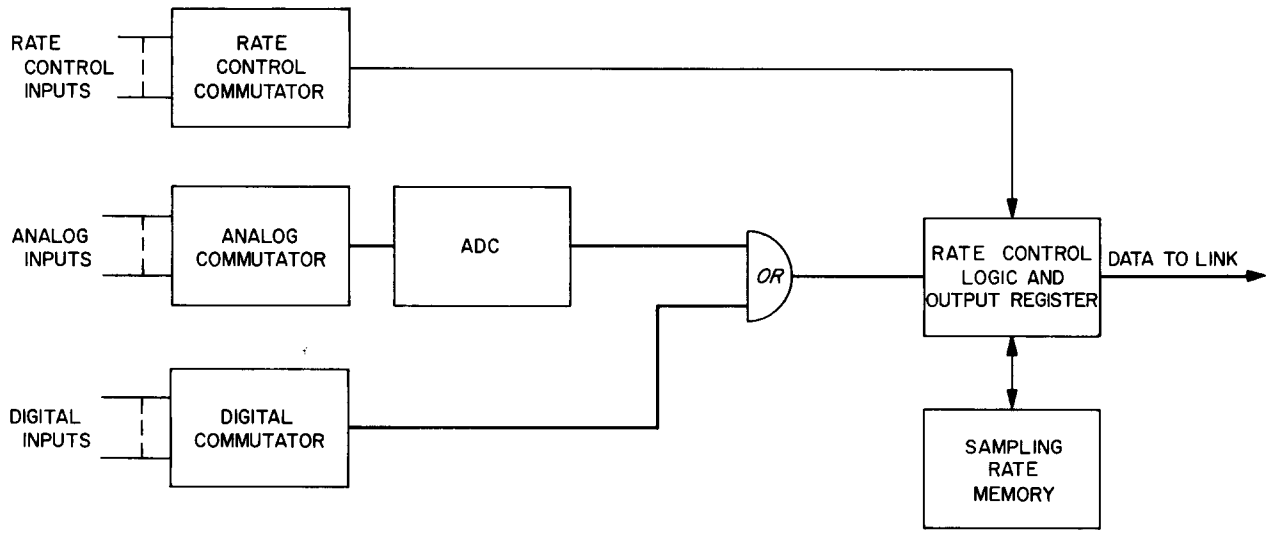

Fig. 7. Subsystem block diagram

UNCLASSIFIED

UNCLASSIFIED

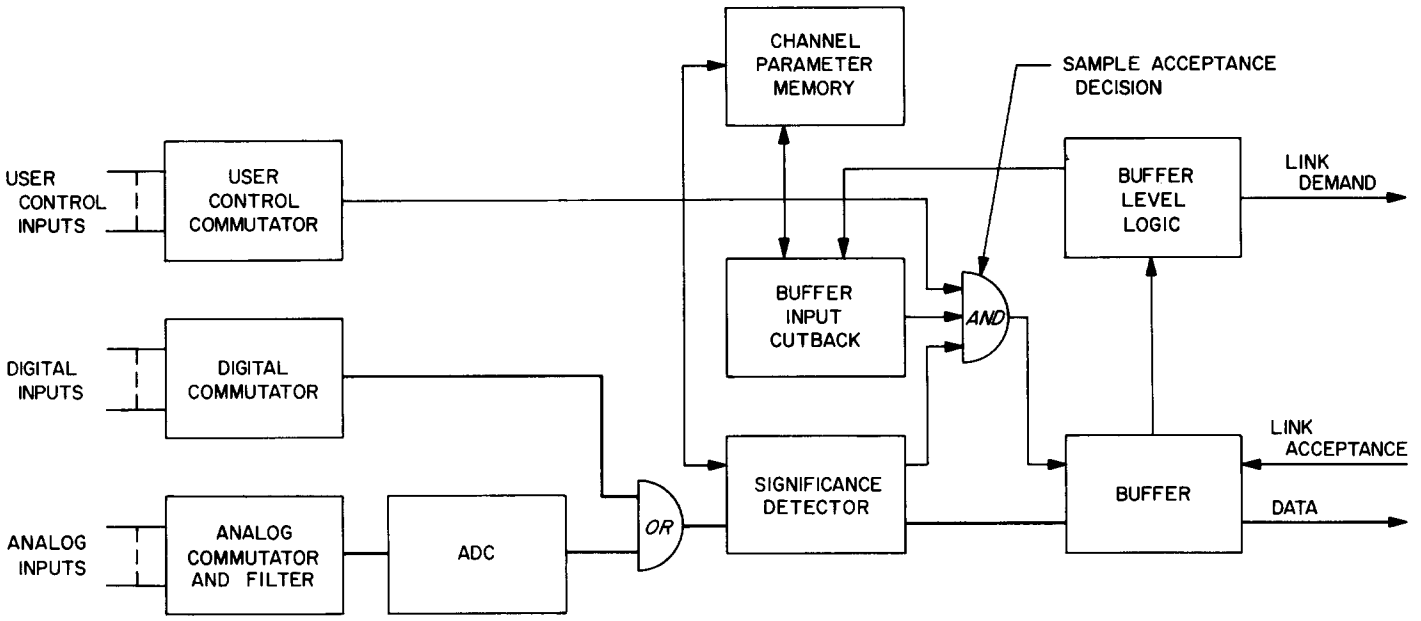

Fig. 8. Block diagram of general data compression system

data that the buffer would normally accept (a reduction of the frequency of acceptance in accord with a selected criterion).

For F2, a volume allotment reduction criterion is used which limits the amount of significant information accepted from each individual F2 channel. The amount of information that may be accepted is a function of:

(1) The weighted volume allotment V_j assigned to each channel

(2) Buffer fullness.

A running sum is kept for each channel of the number of samples stored in the buffer; in this sum each sample is given a weight roughly proportional to the buffer fullness at the time that sample was accepted into the buffer. Thus, a channel that has n samples in the buffer which were accepted while the buffer was nearly empty will have a lower sum than another channel with n samples in the buffer that were accepted when the buffer was ¾ full.

As each sample is processed to determine significance, V_j and the running sum for that channel are brought out from the channel parameter memory and compared. The sample can be accepted only if the running sum is less than the allotment. The specific criterion for acceptance is

$$V_j > \sum_z (N_j)_z W_z$$

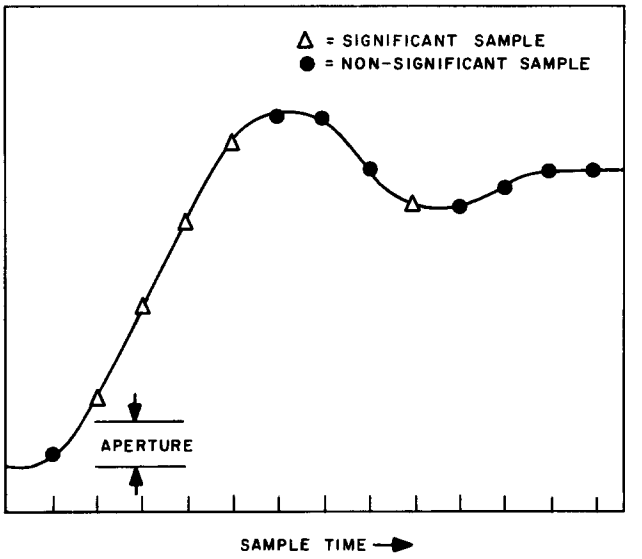

Fig. 9. Waveform sampling by a zero-order comparator

where

V_j is a two-bit code programmed for the jth channel; the programmed value is one of the following four: 1, 2, 4 and 7.

$(N_j)_z$ is the number of buffer samples for the jth channel that entered the buffer when it was within a certain fullness zone Z.

UNCLASSIFIED

UNCLASSIFIED

W_Z is the weighting given when the buffer is in fullness zone Z;

W_Z is a three-bit code having the following values:

W_Z	*Buffer fullness*
1/16	Empty to 1/8 full
1/8	1/8 full to 3/4 full
1/4	3/4 full to 7/8 full
1/2	7/8 full to 15/16 full
1	15/16 full to totally full

Each sample that is accepted has the current W_Z value stored with it in the buffer. As soon as V_j has been compared with the sum, the sum is updated by adding W_Z if there was acceptance and/or subtracting the W_Z value stored with any sample of this channel that left the buffer during the last scanning period. A typical example of the updating of a running sum during periods of buffer level changes is shown in Table 2; cutoff of the channel occurs momentarily in this example.

To ensure that the buffer does not overflow, the average assigned value of V_j must be no greater than 3.375.

Minimum time delay path. The minimum time delay (MTD) feature is provided to permit a small amount of significant data to bypass the buffer and be sent in real-time. This feature is unique to the F2 subsystem. It is required because most operational measurements are of immediate importance and cannot tolerate buffer delays inherent to a data-compression system.

The MTD path will accept a sample at the start of channel activity and periodically during that activity. The MTD sampling criterion is based upon a time frame which is programmed for each channel and is 84, 168, 336, or 672 sec. The exact criterion is that:

(1) If there were no zero-order significant samples during the previous time frame and there is one or more zero-order significant samples in the present time frame (i.e., channel activity is starting), the first significant sample plus one sample (whether significant or not) at the end of the present time frame will be sent.

Table 2. Example of running-sum fluctuations and cutoff of a channel during periods of buffer level changes ($V_j = 4$)

Buffer fullness zone	Present buffer weighting factor W_Z	Event		Buffer weighting factor W_Z of transmitted sample	Running sum for jth channel Σ_j
		Acceptance of sample from jth channel	Transmission of sample from jth channel		
0 to 1/8 full	1/16	X			1/16
		X			1/8
1/8 to 3/4 full	1/8	X			1/4
		X			3/8
		X			1/2
3/4 to 1/8 full	1/4	X			3/4
7/8 to 15/16 full	1/2	X			1 1/4
			X	1/16	1 3/16
		X			1 11/16
		X	X	1/16	2 1/8
		X	X	1/8	2 1/2
15/16 to full	1	X			3 1/2
			X	1/8	3 3/8
			X	1/8	3 1/4
		X			4 1/4
		Cutoff	X	1/4	4
7/8 to 15/16 full	1/2	Cutoff	X	1/2	3 1/2
		X	X	1/2	3 1/2
			X	1/2	3
1/8 to 3/4 full	1/8		X	1/2	2 1/2
			X	1	1 1/2
			X	1	1/2
			X	1/2	0
		X			1/8

CONFIDENTIAL UNCLASSIFIED

UNCLASSIFIED

(2) If there are significant samples both in the previous time frame and in this time frame, one sample (whether significant or not) at the end of the time frame will be sent.

(3) If there is no significant sample in the present time frame, no sample will be sent during or at the end of the frame.

An example of a typical waveform and the resulting samples sent by the MTD path and the data-compression path (provided there is no buffer cutback) is shown in Fig. 10.

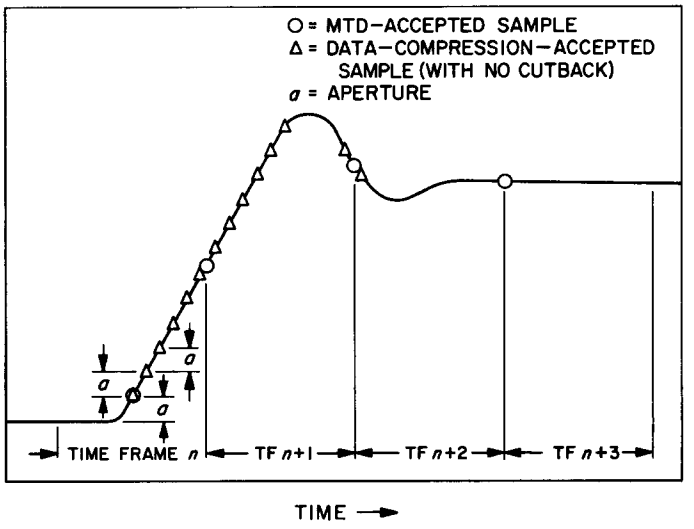

Fig. 10. MTD samples and data-compression samples for a typical waveform

c. F3 high-speed and F3 low-speed subsystems. The F3HS and F3LS subsystems operate identically and differ only in size and sampling rate. F3HS has 30 data channels and 2 time channels while F3LS has 254 data channels and 2 time channels. They are data-compressive subsystems (Fig. 6) in which the significance detector is a zero-order comparator and the buffer input cutback scheme is the reduction of channel sampling rate with a limited reduction of channel allotment of buffer volume provided to prevent a noisy channel from filling the buffer. The reduction of channel allotment is identical to that used in the F2 subsystem. It is used only as a back-up subsystem in the F3 subsystems.

Reduction of sampling rate. The reduction of channel sampling rate is the number of significant samples accepted by the F3HS and F3LS buffers from each channel.

The sampling rate of a given channel depends upon three factors:

(1) The buffer fullness level; there are four zones of fullness:

Zone	*Fullness*
Z_1	0 to ¼
Z_2	¼ to ½
Z_3	½ to ¾
Z_4	¾ to full

(2) A three-bit programmed parameter that relates the maximum sampling rate of each channel to the commutator scan rate; this relationship for the jth channel is

$$(R_j)_{max} = R_c \cdot \left(\frac{1}{2}\right)^{n_j}$$

where

$$R_c = \text{commutator rate} = \begin{cases} 256 \text{ scans/sec for F3HS} \\ 1 \text{ scan /sec for F3LS} \end{cases}$$

n_j = programmed parameter = 0, 1, 2, 3, 4, 5, 6, or 7.

(3) Three one-bit programmed parameters (C_{j1}, C_{j2}, and C_{j3}) indicating whether or not rate cutback is to occur for the jth channel at the first, second, and/or third change of buffer zones (i.e., at ¼, ½, and ¾ fullness levels). If a C_j is a logic 0, no cutback will occur at the corresponding zone transition; if a C_j is a logic 1, a rate cutback equal to ½ will occur at the zone transition. Thus, if $C_{j2} = 1$ (corresponding to the transition at ½ buffer fullness), the sampling rate in zone Z_3 is ½ that in zone Z_2.

From the above discussion, it can be seen that the sampling rate of the jth channel R_j corresponding to buffer fullness zones Z_1, Z_2, Z_3, and Z_4 are

$$(R_j)_{Z1} = (R_j)_{max}$$

$$(R_j)_{Z2} = (R_j)_{Z1} \times \begin{cases} ½ \text{ if } C_{j1} = 1 \\ 1 \text{ if } C_{j1} = 0 \end{cases}$$

$$(R_j)_{Z3} = (R_j)_{Z2} \times \begin{cases} ½ \text{ if } C_{j2} = 1 \\ 1 \text{ if } C_{j2} = 0 \end{cases}$$

$$(R_j)_{Z4} = (R_j)_{Z3} \times \begin{cases} ½ \text{ if } C_{j3} = 1 \\ 1 \text{ if } C_{j3} = 0 \end{cases}$$

UNCLASSIFIED

UNCLASSIFIED

There are only eight possible rate cutback profiles corresponding to the possible combinations of the three cutback parameters (C_{j1}, C_{j2}, and C_{j3}). These are shown in Fig. 11.

d. Peripheral modules. The peripheral modules shown in Fig. 6 are the link allotment, command reprogram, and the central timing modules.

The link allotment module divides the available bandwidth among the four subsystems according to the priority of each subsystem and the amount of activity that is occurring within each subsystem (i.e., the fullness level of each subsystem buffer). The command reprogram module provides for commanded confidence sampling and permits the modifying of the programmed parameters for any channel of any of the four subsystems. The central timing generator module performs all timing functions that are common among the four subsystems.

e. Selected hardware

Logic elements. The Fairchild DTμL 9040 low-power integrated circuit logic family was chosen for this design. These elements have power requirements of less than 1 mw per gate, and less than 4 mw per flip-flop. The family is capable of operating at clock rates above 2 Mc.

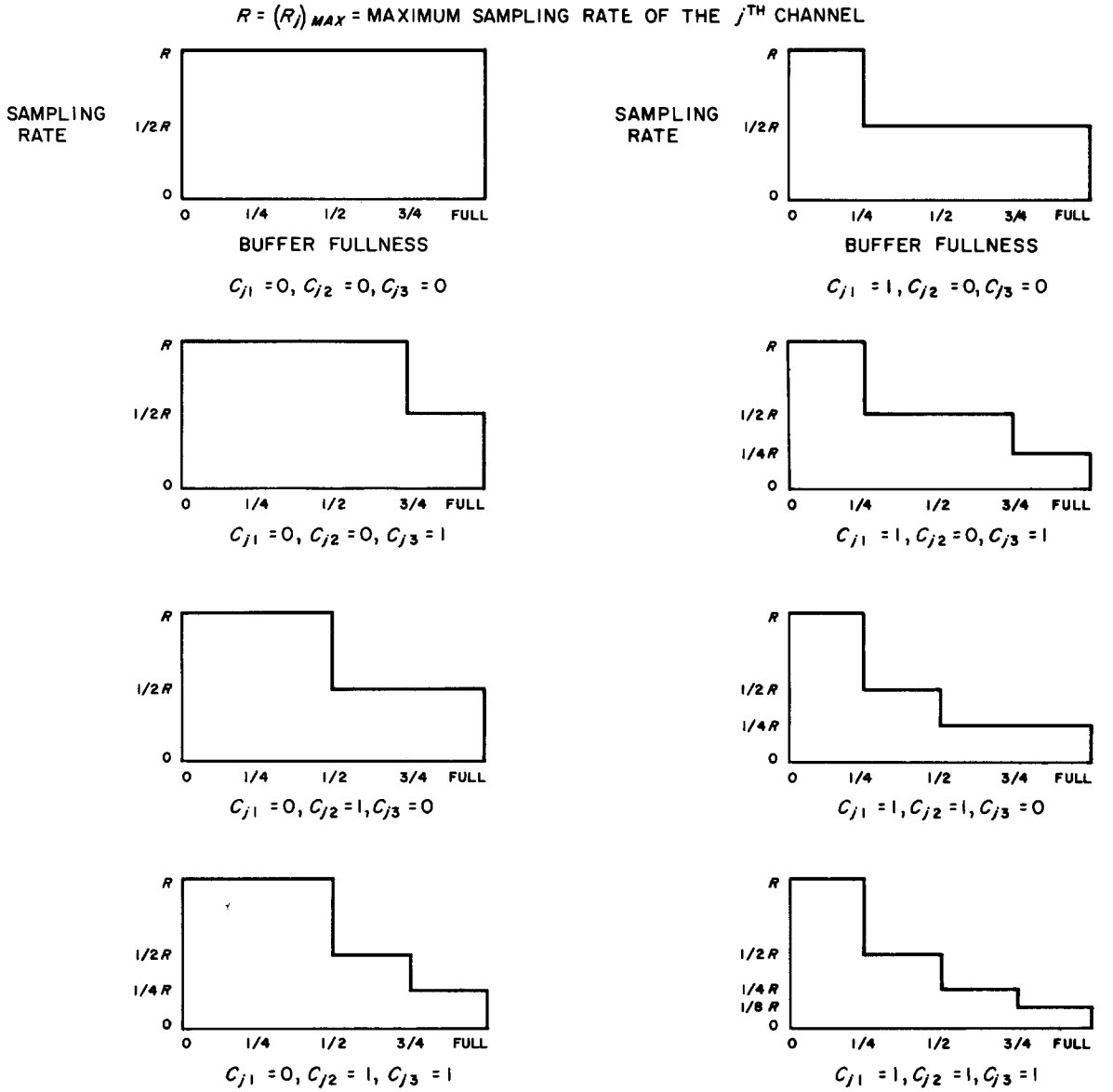
R = (Rj) MAX = MAXIMUM SAMPLING RATE OF THE jTH CHANNEL
SAMPLING RATE
R
1/2R
1/4R
1/8R
0
0
1/4
1/2
3/4
FULL
BUFFER FULLNESS
Cj1 = 0, Cj2 = 0, Cj3 = 0
Cj1 = 1, Cj2 = 0, Cj3 = 0
Cj1 = 0, Cj2 = 0, Cj3 = 1
Cj1 = 1, Cj2 = 0, Cj3 = 1
Cj1 = 0, Cj2 = 1, Cj3 = 0
Cj1 = 1, Cj2 = 1, Cj3 = 0
Cj1 = 0, Cj2 = 1, Cj3 = 1
Cj1 = 1, Cj2 = 1, Cj3 = 1

Fig. 11. Rate cutback profiles for all combinations of C_j parameters

UNCLASSIFIED

UNCLASSIFIED
CONFIDENTIAL

Commutator switches. An MOS integrated circuit commutator is being developed for the EDHS-type application. There are 8 switching channels driven by an 8-stage ring counter integrated into one standard integrated circuit flat pack. Power consumption is 50 mw per flat pack.

Analog-to-digital converter. A microminiature analog-to-digital converter development has been conducted for JPL by the Autonetic Division of North American Aviation, Inc. The resulting prototype ADC proved the feasibility of such a venture, although it did not meet all of the requirements for the EDHS. The unit built had a 9-bit capability, a word rate in excess of 8500 words/sec, and was in three nonstandard flat packs ($1.75 \times 1.10 \times 0.1$ in.). Power consumption is less than 1 w, and shows promise of being reduced below 500 mw.

Memories. A memory technology has been developed by Librascope Division of General Precision, Inc., utilizing a woven plated wire memory element. Such a memory with a 1024×20 capacity is presently being developed for JPL by Librascope. The package for this memory is $6 \times 4 \times 1¼$ in. and the memory weight is approximately 1 lb. Power consumption is less than 275 mw in operation, and less than 50 mw in standby. This memory development is directly applicable to the EDHS.

Packaging. The packaging scheme utilizes the stick modules developed at JPL. The stick modules of interest are $6 \times 1 \times ¼$ in. and can hold up to 14 of the standard 14 lead integrated circuit flat packs. Up to 20 of these sticks will fit into a single $6 \times 6 \times 1¼$ in. *Mariner C* subchassis.

f. Weight, power, and volume estimates. The weight, power, and volume estimates for the EDHS and its subsystems, under present technology are as follows:

Subsystem	Weight, lb	Volume (*Mariner C* subchassis)	Power, w
F1	1.49	0.85	1.21
F2	11.08	8.20	6.94
F3HS	8.87	6.25	4.32
F3LS	12.05	8.85	9.31
Peripheral modules	1.88	1.20	0.95
EDHS totals	35.37	25.35	22.73

With quickly forthcoming technology advances due to large-scale integration, significant savings can shortly be realized in the area of weight and volume estimates. As an example, by employing 8-bit shift registers integrated onto a single chip instead of 8 separate flip-flops, the volume estimate is reduced to 20 *Mariner C* subchassis and the weight is reduced to 27.8 lb.

Glossary

Absolute rate commutator (ARC)	A commutator which operates at a constant rate throughout a given mission.
Accepted data	A sample that satisfies all data-compression criteria and hence is entered into the buffer.
Channel	The communication medium between a measurement sensor and the data handling system; this is not to be confused with "link."
Channel sampling rate	The rate at which a specific channel is sampled.
Digitization rate	The rate of digitization of the analog-to-digital converter; for the EDHS, this rate equals the channel sampling rate of a given subsystem times the number of channels in the subsystem.
Information	Data that are significant (see "significant data").
Link	The communication medium between the spacecraft and the Earth. This is not to be confused with "channel."
Module	A group of components (e.g., flip-flops, gate, commutator decks, resistors, etc.) that perform a function; a circuit. There are three prime modules in the EDHS—the central timing generator, the command reprogrammer, and the link allotment.
Profile	A cluster of data points representing a measurement waveform.
Significant data	Data that are of interest to the intended data user. Ideally, significant data are unexpected data; in practice there are hardware limitations in modeling the expected data profiles.

UNCLASSIFIED

UNCLASSIFIED

2. High-Impact 20-w TWT Amplifier Development

a. Introduction. The traveling wave tube (TWT) RF power amplifier is the present choice for spacecraft applications where communications requirements call for power levels in excess of solid-state capabilities. None of the competing devices offer the combination of gain, bandwidth, efficiency, ruggedness, and reliability inherent in the metal-ceramic TWT. Consideration of the probable RF power requirements for planetary lander capsules has therefore necessitated the development of a high-impact 20-w TWT amplifier. The objectives of the development are: (1) development of high-impact technology, and (2) demonstration of a flight prototype 20-w TWT amplifier with the ability to survive 10,000-*g* 1-msec shocks in any orientation.

Proposals were solicited for this development in June 1965. On the basis of technical competence illustrated by the proposal and existing rugged design which could be utilized, a contract was awarded to the Watkins-Johnson Company, in January 1966. The amplifier will consist of a TWT, power supply and output RF filter in a single package. The specifications are as follows:

Weight	7 lb
Operational life	20,000 hr or more
Input power	70 w or less
Input voltage	+25 to +50 VDC
RF output	+43 dbm (20 w)
RF input (drive)	+18 dbm, or less
Frequency range	2.29 to 2.30 GHz

b. Design approach. In order to achieve the above goals with a reasonable time and cost, the following approach is being used: the TWT, power supply, and RF filter will be designed and constructed, with a minimum of predesign testing, and shock-tested. This process will be repeated if the shock reveals deficiencies. The amplifier will be designed, integrating the components into a single package, and then shock-tested. This process will also be repeated until an acceptable design is achieved. Type-approval tests will include all *Mariner C* tests and sterilization qualification. Finally the amplifier will be life-tested.

c. TWT design considerations. TWT design is to be based on the WJ-274 TWT with modifications to meet the shock requirement. The areas of primary concern are the helix and electron gun.

In a TWT, amplification is caused by the interaction of fields generated by the desired signal on a slow wave structure and an electron beam. The most efficient structure yet developed for a TWT in the power class being considered is a helix with the electron beam traveling axially down the helix center. Ideally, the helix should be suspended in free space. Since this is structurally impractical, the helix is supported by three rods or wedges spaced around the outside of the helix at 120-deg intervals.

Wedges were chosen to support the helix for this development, since a much greater support-area/mass ratio results. Helix support wedges are normally made of either beryllia or alumina ceramic. Beryllia is often used because of its superior heat conduction. Alumina was tentatively chosen for this development because of its superior strength, and because the heat dissipation requirements are not critical at the power level in question.

Because of the shock requirement it is necessary to bond the helix to the support wedges. This bond may be achieved by metalizing the wedges at the points where the helix touches and brazing. Since the metalizing must be carefully controlled to prevent shorts between turns or excessive loading of the helix, this is an extremely difficult manufacturing operation. An alternate method uses a glass glaze which bonds to the entire length of the support and each turn of the helix. A much more uniform helix having better electrical characteristics results. The glaze bond is weaker than the braze bond. Since the required bond strength was not known, the type of bond was to be chosen after shock testing.

The cross-section of the helix wire may be either round (wire helix) or rectangular (tape helix). The tape helix presents a greater bonding area to the support rod and therefore would seem the stronger design. If the increased strength is not required, a wire helix is preferred, due to the larger body of design data available. Since the required strength was not known, this choice was also deferred until after shock testing.

The TWT electron gun is considered to be the major TWT design problem area. The electron emitting cathode is operated at high temperature to achieve the desired electron emission. The cathode supports conduct heat away from the cathode and reduce the TWT efficiency. In a normal TWT the cathode supports are long, slender rods or crossed wires. This type of structure has a high thermal impedance, but is not readily adaptable to high-shock use. A drawn cone of strong, low heat conductivity material was proposed to support the cathode for this

CONFIDENTIAL UNCLASSIFIED

UNCLASSIFIED

development. Static calculations and model loading tests indicate that the required rigidity under 10,000-*g* loading is provided by this design. Since the other elements of the TWT electron gun are not required to operate at a high temperature, a straightforward "beefing up" process is used for 10,000-*g* design.

d. Power supply, RF filter, and system design considerations. The TWT power supply will be made up of several solid potted modules. The electrical circuit will be a modification of a power supply developed for an earlier program. The power supply design effort will consist of extending the input voltage range to the +25 to +50-v JPL requirement, and repackaging to meet the 10,000-*g* shock requirement. The shock requirement is expected to limit the maximum module size.

The RF filter is to be provided by RANTEC. The electrical requirements are met by units already in production. A high-level design effort will be required to meet the 10,000-*g* shock requirement without sacrificing any of the electrical qualities. Extreme rigidity is required in a distributed reactance filter, since any deformation will cause detuning. Distributed reactances must be used at the frequencies in question, since low-loss lumped reactance components of the required values do not exist. If possible, the requirements will be met by rugged construction and electrical designs which avoid unsupported sections. A filter filled with solid dielectric would be sufficiently rugged, but dielectric losses would make the efficiency requirement almost impossible to meet. The solid dielectric filled filter will be used if other approaches fail.

The amplifier will be packaged as a single unit. Package design will remain fluid until more is known about the amplifier components. A cast or machined block of aluminum or magnesium; with individual "pockets" providing support on five sides for the tube, filter, and power supply modules, is considered the most likely design at this time.

e. Progress. Initial TWT design is progressing satisfactorily. The following tests of suspected problem areas have been conducted:

(1) Magnet stability after three 145°C 36-hr sterilization cycles.

(2) 10,000-*g* shock tests of: 4 alternate helix and support designs, the Watkins-Johnson standard input-output window design, and the half-tube magnetic circuits.

(3) Magnetic leakage field plot.

The magnetic sterilization stability test resulted in only a 1.84% field change. This is an acceptable level of stability, and no magnetic design changes are required by sterilization.

The 10,000-*g* shock tests revealed a great deal of data. Only tape helices were able to withstand the 10,000-*g* shocks. Wire helices failed at, or below, the 3,200-*g* level. The difference in shock resistance is attributed to the greater bonding area available on the flat tape helix. The glaze bond proved capable of surviving the 10,000-*g* shock and is preferred because of its electrical and production characteristics. Alumina will probably be the wedge support material, although beryllia was not disqualified by the shock tests.

The input-output window test was inconclusive, because the tube bodies failed. The mass of the platinum-cobalt magnets sheared the bond to the aluminum fixture, and the stainless steel internal tube envelope. This unexpected failure will direct design attention to magnet support in the future to prevent failure in this area. The magnetic field distribution in the tube half-bodies was measured after the shock test. Discontinuities were found where the tube structure failed under shock tests, but the field was not changed in other sections. From this result it seems safe to conclude that 10,000-*g* shocks do not degrade properly mounted platinum-cobalt magnets.

The magnetic leakage test was performed on a TWT with a magnetic design similar to that proposed for the high-impact amplifier. The maximum leakage field was 17 gamma at 3 ft. The tube was tested as received, after exposure to a 25-gauss 60-cps AC demagnetizing field, and after exposure to a 25-gauss DC magnetizing field along the tube axis. Less than 2-gamma change was measured in any plane. Since the field is regular and stable, compensation should be possible. The decision has been made not to shield the amplifier. No further effort toward magnetic leakage field control will be expended until a clarification of magnetic requirements for a specific application is received.

A breadboard power supply was constructed, and operation over the +25 to +50-v range was achieved. The efficiency of the power supply was lowered by the modification that extended the input voltage range. This must be corrected. It was determined in the first program review that the weight of the amplifier was above specification limit, with the added weight of the modified power supply design, and the including of heat sinks for the power semiconductors. This situation may be partially relieved by positioning semiconductors in the potted modules so

UNCLASSIFIED

UNCLASSIFIED

that the amplifier case may be used directly for heat sinking.

The RF filter specification has been completed, and work will start on this component in the near future.

3. S-Band TWT Evaluation

a. Introduction. A test unit has been established to evaluate a number of RF power amplifiers for possible *Voyager* and other future spacecraft applications. The amplifiers will be evaluated for performance under those conditions of temperature, vibration, and shock set forth in JPL Specification 30250B for the type-approval testing of *Mariner C* flight equipment. The RF power amplifiers will also undergo a life test. Each of the RF power amplifiers will have undergone bench testing to determine their acceptability under static conditions prior to environmental testing.

The major task will be to design and fabricate suitable test sets which will power, protect and evaluate those RF amplifiers under environmental and life tests.

In order to afford the utmost in protection to the RF power amplifier (in some instances a one-of-a-kind item) the test sets must be extremely reliable, operating without attention for long periods of time. Their evaluation information must be able to interface with the existing recording facilities in the environmental facility. Any failure of the RF power amplifier, its test set, or the environment in which either is operating must result in a complete shutdown of all power.

b. Design. The test set described here was designed around the Hughes 394-H 20-w S-band TWT, which had been previously bench-tested and found to operate satisfactorily.

It was planned to design protection for the following:

(1) Loss of vacuum in the test chamber

(2) Overtemperature or undertemperature in the test chamber

(3) Loss of prime power to the test set

(4) Excessive helix current

(5) Loss of RF power

(6) Overvoltage or undervoltage at the TWT's second anode

It was also planned to evaluate the TWT for constancy of output and the degree of phase jitter introduced by environments of heat, cold, vibration, and shock.

The plan included semiautomatic instrumentation to provide analog recordings of S-band power input, S-band power output, phase jitter and amplitude modulation caused by certain types of environment. Visual monitoring of the tube operating parameters was to be available from panel-mounted meters.

c. Mechanization. Shown in Fig. 12 is a block diagram of the entire system, consisting of the test set, a CEC 5-124 recording oscillograph, and an Ampex FR-600 high-resolution recorder.

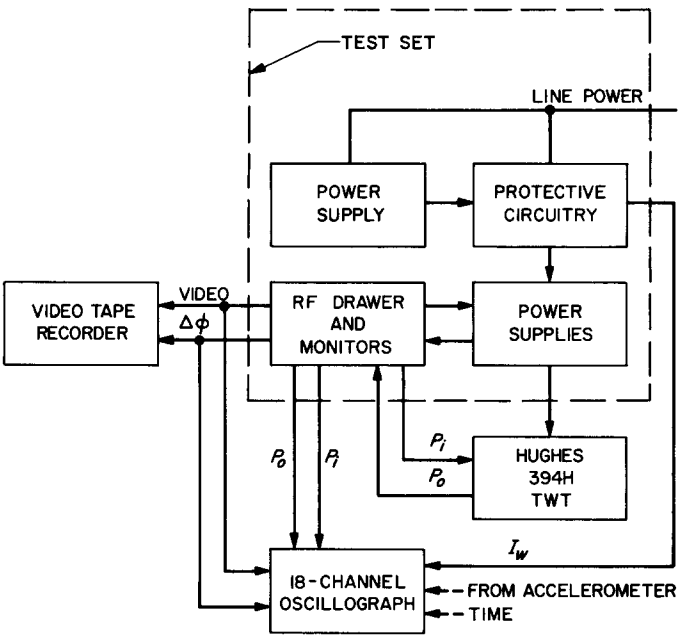

Fig. 12. Test evaluation system for the Hughes 394-H TWT

The test set consists of a DC power and protective circuitry section in one rack, with RF generating and monitoring sections in a second rack. Fig. 13 shows the completed test set. The DC power section is conventional except for the TWT filament supply, which was designed to be isolated from the system ground.

The protective circuitry (Fig. 14) is made up of both commercial and JPL-built modules. It employs commercial protection/control circuitry to guard against the loss of vacuum and overtemperature/undertemperature variations. A sensor for the loss of vacuum provides an actuating voltage to a prime power "shutdown" relay in the

UNCLASSIFIED

UNCLASSIFIED

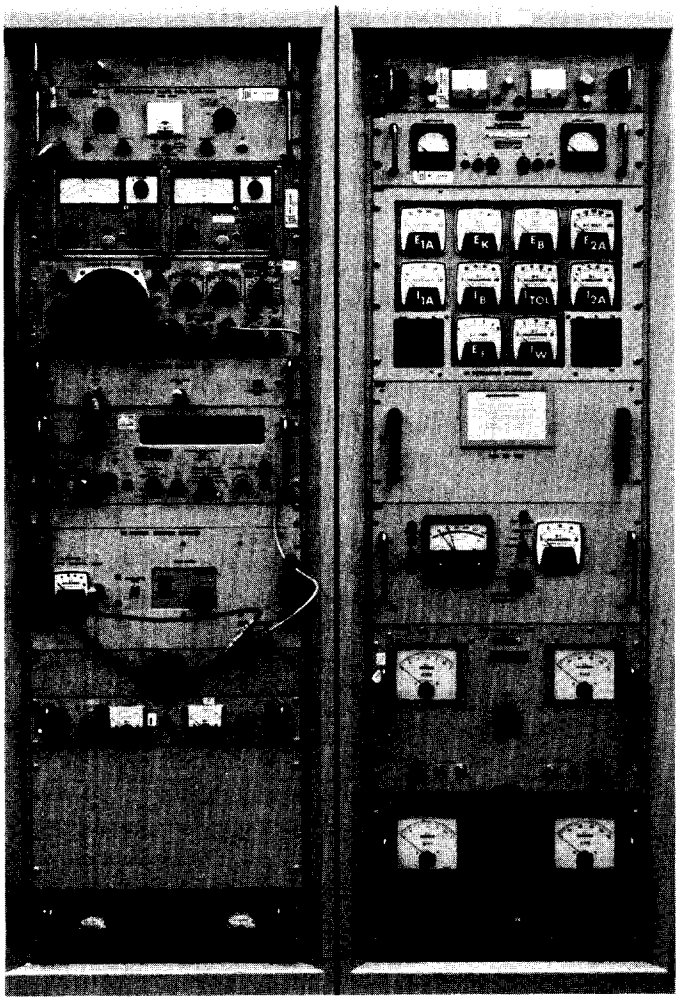

Fig. 13. Test set for the Hughes 394-H TWT

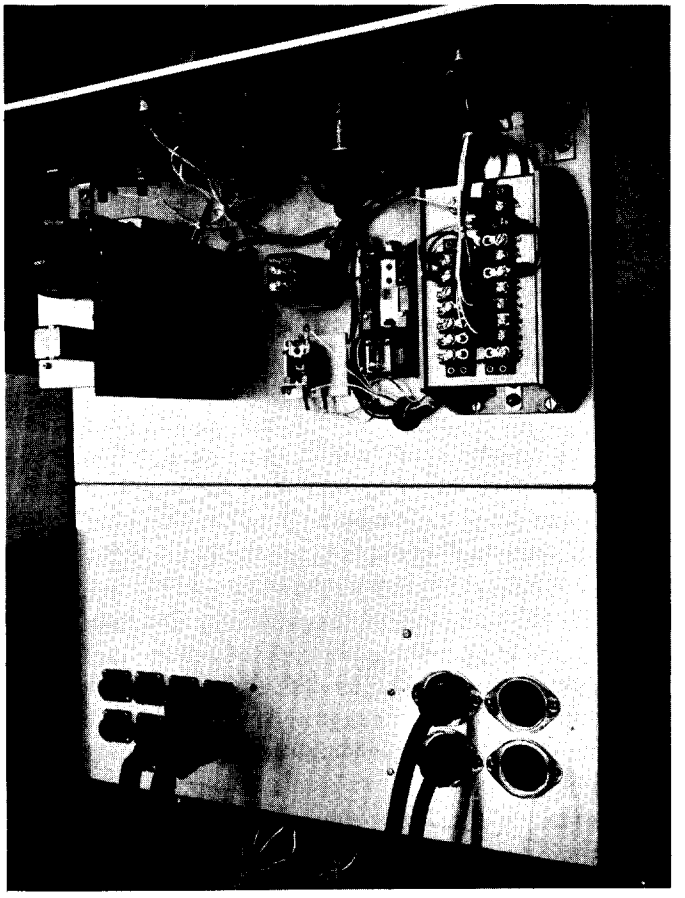

Fig. 14. Protective circuitry

test set protective circuitry assembly. The overtemperature/undertemperature protection is obtained by the use of a copper-constantan thermocouple, which provides temperature information to an Assembly Products Model 907B control unit and its associated optical meter-relay. Low and high temperature limits are set by the meter-relay; a temperature variation of ±4 deg relative to a predetermined setting provides an actuating signal to the prime power shutdown relay. Indicator lamps on the panel of the protective circuitry assembly indicate whether the shutdown occurred due to an excessively high or an excessively low temperature.

The remainder of the protective circuitry consists of relays and solid state amplifier/trigger circuits integrated to provide prime power shutdown when the following occurs:

(1) When the TWT helix current exceeds 15 ma

(2) When the 2295-Mc RF output power drops off 1.4 db or more

(3) When the prime line power fails

(4) When the TWT second anode voltage varies in excess of ±20 v

When any of the foregoing types of failure occurs, a battery-operated bell sounds. Included in the protective circuitry is a "simulated failure" provision, which checks out certain of the protective devices without disturbing the TWT's normal operation.

Fig. 15 is a block diagram of the 2295-Mc RF generating and measurement circuitry, and Fig. 16 is a photograph of the RF measurement drawer. Of paramount importance is the phase modulation generated by the TWT under test throughout the range of specified environment. In order to evaluate this, the input phase is compared with the output phase in an S-band phase detector. The phase

UNCLASSIFIED

UNCLASSIFIED

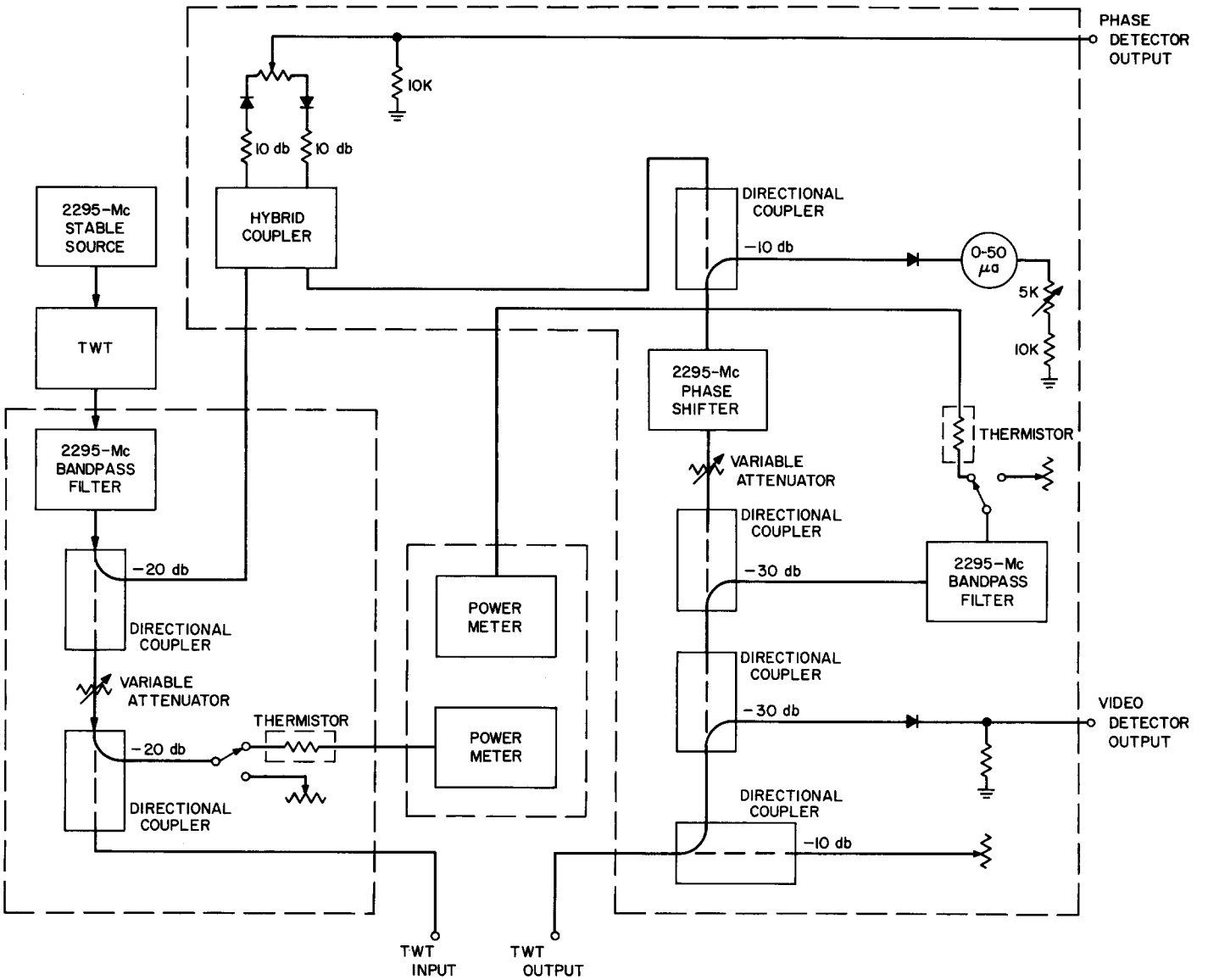

Fig. 15. RF generating and measurement circuitry

detector (acting as a bridge) is balanced prior to an environmental test, using a calibrated S-band phase shifter. This detector, having been previously calibrated at various points out to ±90 deg, will produce a DC voltage proportional to the phase error developed by the TWT during the test.

This system has two distinct advantages over the phase-locked receiver. They are:

(1) Detection of phase jitter can be made by comparing the output signal to the input signal, because any phase jitter present at the detector output will be that caused by the device under test, since residual phase jitter from the drive source is cancelled.

(2) Since there is no phase tracking involved in this S-band phase detector, low-frequency phase error components will not be tracked out, as they would in a conventional DSIF-type receiver.

As long as the ratio of signal amplitude to reference amplitude is 10:1 (or greater) in the phase detector, the variation in phase is approximately 1 deg/db signal input change. With design input power the phase detector develops 450 mv peak-to-peak, and has a slope of 3.6 mv per degree of phase shift out to ±30 deg.

UNCLASSIFIED

UNCLASSIFIED

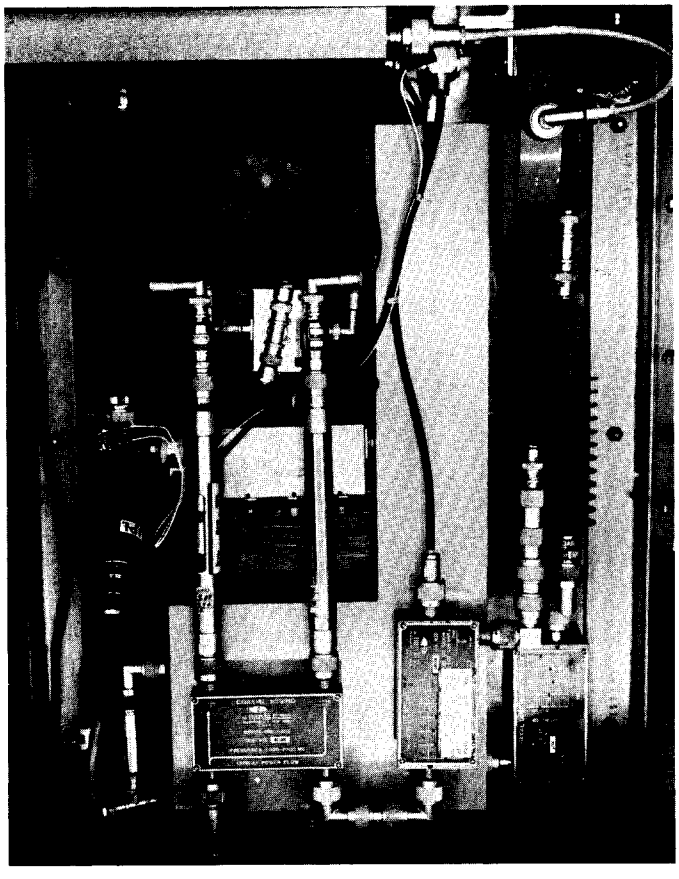

Fig. 16. RF measurement drawer

Fig. 17 is a photograph of the Hughes 394-H TWT mounted on its test fixture. Tests are scheduled for May 1966.

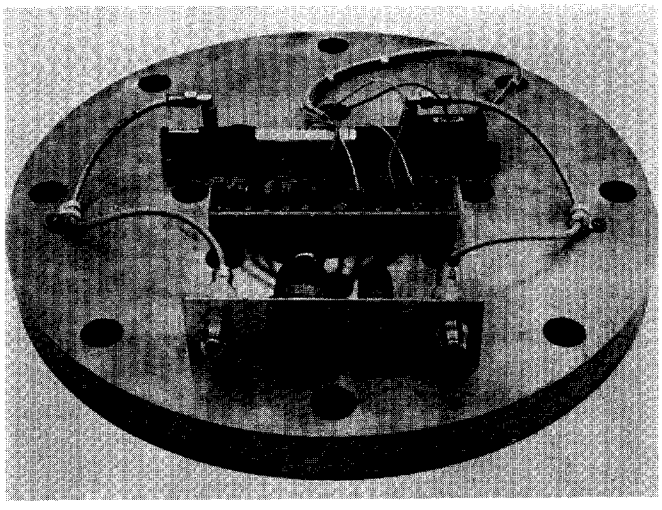

Fig. 17. Hughes 394-H TWT mounted on its test fixture

The instrumentation of the TWT is roughly of two types; (1) direct visual indication (meters, oscilloscopes, etc., which must be read periodically) and (2) an analog recording of performance of selected parameters. Visual indications include all DC voltages applied to the TWT and the resulting current flows.

A rectified sample of the TWT output signal is available for high-resolution magnetic recording, and/or analog oscillographic recording. The output of the phase detector, RF power input, RF power output, acceleration and time are also recorded on an oscillograph during vibration and shock tests. Only direct visual indications are taken during temperature tests.

References

1. "Solar Proton Manual," Frank B. McDonald, Ed., NASA TR R-169, December 1963.

2. "Range-Energy Tables," University of California Radiation Laboratory Report No. 2301, Berkeley, California, 1954.

UNCLASSIFIED

UNCLASSIFIED

IV. Future Projects

A. Introduction

The Future Projects Office is responsible for the direction, sponsorship and the origination of advanced mission and future project studies in the areas of interest and applicability to the Laboratory.

The objective of this effort is to ensure that the preliminary technical information and plans for the various potential missions, together with the associated information on spacecraft systems, instrumentation systems, launching vehicle systems, resources, and schedule be available as required. This preliminary mission study information will be used primarily for defining specific flight mission programs and as generalized guidance for the Laboratory research and advanced development programs.

Each study conducted by this Future Projects Office has been, and will continue to be, documented in a formal final report. A summary of the results of each such study including reference to the final report for additional details will appear in this section when appropriate.

UNCLASSIFIED